

1  
2  
3  
4  
5  
6  
7  
8  
9  
10  
11  
12  
13  
14  
15  
16  
17  
18  
19  
20

RUNNING HEAD: USING *GBS* TO RESOLVE RECENT PLANT RADIATIONS

**Resolving Recent Plant Radiations: Power and Robustness of Genotyping-  
by-Sequencing**

Mario Fernández-Mazuecos<sup>1\*</sup>, Greg Mellers<sup>1</sup>, Beatriz Vigalondo<sup>2</sup>, Llorenç Sáez<sup>3</sup>, Pablo  
Vargas<sup>4</sup>, Beverley J. Glover<sup>1</sup>

<sup>1</sup>*Department of Plant Sciences, University of Cambridge, Cambridge CB2 3EA, UK*

<sup>2</sup>*Departamento de Biología (Botánica), Facultad de Ciencias, Universidad Autónoma de Madrid, 28049  
Madrid, Spain*

<sup>3</sup>*Departament de Biologia Animal, Biologia Vegetal i Ecologia, Unitat de Botànica, Facultat de Ciències,  
Universitat Autònoma de Barcelona, 08193 Bellaterra, Barcelona, Spain*

<sup>4</sup>*Real Jardín Botánico (RJB-CSIC), Plaza de Murillo 2, 28014 Madrid, Spain*

*\*Correspondence to be sent to: Mario Fernández-Mazuecos. Real Jardín Botánico (RJB-CSIC), Plaza de  
Murillo 2, 28014 Madrid, Spain; Tel.: +34 914203017. E-mail: mfmazuecos@rjb.csic.es.*

21           *Abstract.*—Disentangling species boundaries and phylogenetic relationships within  
22 recent evolutionary radiations is a challenge due to the poor morphological differentiation  
23 and low genetic divergence between species, frequently accompanied by phenotypic  
24 convergence, inter-specific gene flow and incomplete lineage sorting. Here we employed a  
25 genotyping-by-sequencing (GBS) approach, in combination with morphometric analyses, to  
26 investigate a small western Mediterranean clade in the flowering plant genus *Linaria* that  
27 radiated in the Quaternary. After confirming the morphological and genetic distinctness of  
28 eight species, we evaluated the relative performances of concatenation and coalescent  
29 methods to resolve phylogenetic relationships. Specifically, we focused on assessing the  
30 robustness of both approaches to variations in the parameter used to estimate sequence  
31 orthology (clustering threshold). Concatenation analyses suffered from strong systematic  
32 bias, as revealed by the high statistical support for multiple alternative topologies depending  
33 on clustering threshold values. By contrast, topologies produced by two coalescent-based  
34 methods (NJ<sub>st</sub>, SVDquartets) were robust to variations in the clustering threshold. Reticulate  
35 evolution may partly explain incongruences between NJ<sub>st</sub>, SVDquartets and concatenated  
36 trees. Integration of morphometric and coalescent-based phylogenetic results revealed (1)  
37 extensive morphological divergence associated with recent splits between geographically  
38 close or sympatric sister species, and (2) morphological convergence in geographically  
39 disjunct species. These patterns are particularly true for floral traits related to pollinator  
40 specialisation, including nectar spur length, tube width and corolla colour, suggesting  
41 pollinator-driven diversification. Given its relatively simple and inexpensive implementation,  
42 GBS is a promising technique for the phylogenetic and systematic study of recent radiations,  
43 but care must be taken to evaluate the robustness of results to variation of data assembly  
44 parameters. [Genotyping-by-sequencing; RAD-Seq; radiation; phylogeny; coalescence;  
45 concatenation; speciation; *Linaria*.]

46

47           Recent evolutionary radiations constitute ideal systems to investigate evolution,  
48 speciation and adaptation (Schluter 2000; Hughes and Eastwood 2006; Seehausen 2006;  
49 Valente et al. 2010; Farrington et al. 2014). To understand the causes and direction of  
50 evolutionary change, robust systematic treatments and well-resolved phylogenies are  
51 required. However, disentangling species boundaries and phylogenetic relationships within  
52 recent evolutionary radiations is a challenge due to the low genetic divergence between  
53 species, frequently accompanied by inter-specific gene flow and incomplete lineage sorting  
54 (ILS) (Shaw 2002; Shaffer and Thomson 2007). This leads to poor resolution, low support  
55 values and short branch lengths in phylogenetic trees, interpreted as signatures of rapid  
56 diversification (Valente et al. 2010; Meiklejohn et al. 2016). Although morphological  
57 diversity may be considerable, the high frequency of phenotypic convergence further  
58 confounds systematics and phylogeny, yet it has high evolutionary interest because it is  
59 potentially informative about recurrent adaptive traits and their molecular basis (e.g. Whittall  
60 et al. 2006; Muschick et al. 2012). Some authors cast doubt on the possibility of resolving  
61 recent radiations in the tree of life because of these difficulties (Vargas and Zardoya 2014),  
62 and even state-of-the-art approaches have methodological challenges to overcome (Harvey et  
63 al. 2016).

64           In plants, classical approaches to phylogenetic analysis are based on a small number  
65 of loci, frequently nuclear ribosomal DNA (nrDNA), plastid DNA (ptDNA) and low-copy  
66 number genes (Sang 2002; Álvarez and Wendel 2003; Shaw et al. 2007). This strategy has  
67 been proven effective to resolve some recent radiations, and is frequently able to recover  
68 major clades and evolutionary patterns (Givnish et al. 2009; Guzmán et al. 2009). However,  
69 incongruence between loci that may result from hybridisation and ILS, amongst other causes,  
70 often brings about uncertainty regarding species boundaries and species-level relationships  
71 (Blanco-Pastor et al. 2012). Under these conditions, the sequencing of a large number of

72 genome-wide genetic markers, accompanied by thorough intra-specific sampling of  
73 individuals, is a requirement to resolve systematic and phylogenetic questions. To achieve  
74 this, several approaches based on next generation sequencing (NGS) have been proposed in  
75 recent years, including sequence capture, transcriptomics and restriction digest-based  
76 methods (Lemmon and Lemmon 2013; McCormack et al. 2013; Harvey et al. 2016).  
77 Restriction digest-based NGS methods comprise a number of procedures, including those  
78 known as restriction-site associated DNA sequencing (RAD-Seq) and genotyping-by-  
79 sequencing (GBS) (van Orsouw et al. 2007; Baird et al. 2008; Davey et al. 2011; Elshire et al.  
80 2011; Peterson et al. 2012; Poland et al. 2012). Despite the plethora of protocols that have  
81 been published, a NGS-based method that is universally and routinely applicable by  
82 systematic biologists is yet to be established as a replacement to conventional phylogenetic  
83 approaches. Such a method should not only be capable of providing genome-wide  
84 phylogenetic information, but should also be cost- and time-effective, involve relatively  
85 simple laboratory protocols, and should not require a sequenced reference genome or  
86 previous genomic information (Lemmon and Lemmon 2013; McCormack et al. 2013).  
87 Ideally, it should also be successful with fragmented DNA available from biological  
88 collections of various ages.

89         In addition to laboratory protocols, uncertainties also remain concerning the  
90 bioinformatic analysis of large numbers of genomic loci with potentially conflicting  
91 phylogenetic signals. The concatenated approach has frequently been favoured because of its  
92 analytical speed (Wagner et al. 2013; Hipp et al. 2014). However, simulation studies show  
93 that, even when analysing thousands of loci, concatenated analysis can produce inconsistent  
94 results in the presence of ILS (Kubatko and Degnan 2007). Species tree methods based on the  
95 multi-species coalescent approach therefore should be preferred to deal with this problem but  
96 they may be computationally intensive (reviewed by Liu et al. 2015). In addition, as for

97 concatenation methods, species tree methods may be inconsistent in the presence of  
98 hybridisation (Solís-Lemus et al. 2016). Coalescent-based phylogenetic network methods,  
99 capable of dealing with gene flow, are even more computationally intensive, but more  
100 efficient implementations of these are currently in development (Solís-Lemus and Ané 2016).

101 Here we have analysed species boundaries, phylogenetic relationships and patterns of  
102 morphological evolution during speciation in a small radiation of flowering plants, the  
103 Iberian clade of *Linaria* subsect. *Versicolores* (Fernández-Mazuecos et al. 2013a). According  
104 to current taxonomic treatments, this clade comprises eight taxa endemic or sub-endemic to  
105 the Iberian Peninsula, in the western Mediterranean biodiversity hotspot (Sáez and Bernal  
106 2009; Vigalondo et al. 2015; Blanca et al. 2017). This clade constitutes an excellent study  
107 system for the understanding of pollinator-driven floral evolution and speciation because it  
108 has high phenotypic diversity in floral traits promoting pollinator specialisation, including  
109 corolla tube width, corolla colour and nectar spur length (Fernández-Mazuecos et al. 2013a).  
110 Nectar spurs in particular have been considered a key evolutionary innovation, promoting  
111 speciation and morphological diversity (Kay et al. 2006; Fernández-Mazuecos and Glover  
112 2017). However, the Iberian clade also displays a number of features that make it a  
113 challenging study case from both a systematic and phylogenetic standpoint (Fernández-  
114 Mazuecos et al. 2013a; Fernández-Mazuecos and Vargas 2015; Vigalondo et al. 2015): (i)  
115 recent and rapid radiation, dated back to the Quaternary; (ii) potential instances of phenotypic  
116 convergence; (iii) incongruence between ptDNA and nrDNA (internal transcribed spacer,  
117 ITS) phylogenies; (iv) inconsistent results between concatenation- and coalescent-based  
118 phylogenies of combined ptDNA+ITS data; and (v) lack of monophyly of intra-specific  
119 samples and extensive sharing of ptDNA haplotypes across species. As a result, previous  
120 attempts to resolve relationships with standard phylogenetic markers were unable to recover a  
121 reliable species-level phylogeny for this clade.

122 To generate genome-wide phylogenetic markers we selected the genotyping-by-  
123 sequencing approach first described by Elshire et al. (2011) as it does not require previous  
124 genomic information and is relatively simple and inexpensive compared to related restriction  
125 digest-based methods. This makes it a good candidate to become a universally applicable  
126 NGS replacement for conventional phylogenetic approaches. This method has recently been  
127 successfully applied to species phylogenetics and species delimitation (Escudero et al. 2014;  
128 Nicotra et al. 2016), but questions remain concerning the analytical approach to GBS data,  
129 such as the treatment of missing data (whether loci with large proportions of missing  
130 sequences should be excluded or not; Roure et al. 2013; Huang and Knowles 2014; Eaton et  
131 al. 2016) or the relative merits of concatenated and coalescent-based approaches to infer  
132 species phylogenies (DaCosta and Sorenson 2016).

133 Our objective was to use both morphometric data and genome-wide genetic markers  
134 generated by GBS in the Iberian clade of *Linaria* subsect. *Versicolores* to: (1) test species  
135 limits, thus achieving a robust systematic treatment; (2) infer a well-supported species  
136 phylogeny comparing the relative performances of concatenation and coalescent-based  
137 methods; (3) analyse the patterns of morphological evolution during speciation, particularly  
138 those potentially linked to pollinator specialisation. The ultimate goal was to establish a  
139 unified approach that allows the resolution of the elusive species limits and phylogenetic  
140 relationships in a recent radiation.

141

## 142 MATERIALS AND METHODS

### 143 *Study System*

144 The eight taxa currently recognised in the Iberian clade of *Linaria* subsect.  
145 *Versicolores* and acronyms used hereafter in this paper are listed in Table 1 (Sáez and Bernal  
146 2009; Vigalondo et al. 2015; Blanca et al. 2017; see Online Appendix 1). One of these taxa

147 has been treated as either a species or a subspecies (*L. salzmännii* or *L. viscosa* subsp.  
148 *spicata*), while the other seven have been consistently treated as species. An additional taxon  
149 has been described, *L. viscosa* subsp. *crassifolia* (CRA) (Sutton 1988), but its taxonomic  
150 status is uncertain (Sáez and Bernal 2009). These taxa inhabit grasslands and open shrubby  
151 formations on soils developed from diverse lithologies. They are endemic to the Iberian  
152 Peninsula, except for SPA, which is also present in southern France. They are diploid species  
153 with chromosome number  $2n=12$  (Sutton 1988; Sáez and Bernal 2009) and genome sizes  
154 around  $2C=1.1$  pg (Castro et al. 2012), and they all seem to be predominantly allogamous  
155 (Valdés 1970; Fernández-Mazuecos M., unpublished data).

156 The Iberian clade has been strongly supported as monophyletic by both concatenated  
157 and coalescent-based analyses of combined ITS and ptDNA sequences, and it is sister to a  
158 mostly North African clade of c. 20 taxa (Fig. S1a; Supplementary Material can be found in  
159 the Dryad data repository at <http://datadryad.org/review?doi=doi:10.5061/dryad.mp818>)  
160 (Fernández-Mazuecos et al. 2013a; Vigalondo et al. 2015). Both the Iberian and North  
161 African clades constitute *Linaria* subsect. *Versicolores*, which is in turn sister to *Linaria*  
162 subsect. *Elegantes* (two species). Both subsections make up *Linaria* sect. *Versicolores*, one of  
163 the major clades of the toadflax genus (Fernández-Mazuecos et al. 2013b). Divergence  
164 between the Iberian and North African clades has been dated back to the Pliocene or early  
165 Quaternary, and speciation of the Iberian clade is estimated to have happened in the late  
166 Quaternary, during the last million years, with high diversification rates (Fig. S1a;  
167 Fernández-Mazuecos and Vargas 2011; Fernández-Mazuecos et al. 2013a; Fernández-  
168 Mazuecos and Vargas 2015). Two major geographically-structured ptDNA lineages have  
169 been detected in the Iberian clade (Fernández-Mazuecos and Vargas 2015).

170

171 *Morphometric Analysis*

172 A morphometric analysis of all taxa included in the Iberian clade was performed  
173 following the methods of our previous study of INC and ONU (Vigalondo et al. 2015). A full  
174 account of methods is found in Online Appendix 2. Specimens were obtained from herbaria  
175 (Online Appendix 1) and from the authors' collections (vouchers in BCB and MA). The  
176 selected characters included 24 quantitative and three qualitative variables (Table S1). Ten to  
177 thirty-three specimens per taxon were analysed and one measure per character per specimen  
178 was taken. Specimens of two different flower colour morphs of SAL (purple and yellow)  
179 were included, as well as three specimens collected in the *locus classicus* of CRA. The final  
180 morphometric dataset included 166 samples.

181 To assess the morphological affinities between specimens and taxa, principal  
182 coordinate analysis (PCoA) was conducted using Gower's coefficient of similarity for mixed  
183 data (Gower 1971). A discriminant function analysis (DFA) was then performed to reveal the  
184 main characters contributing to the morphological differentiation of taxa and to test the  
185 assignment of specimens to taxa using a cross-validation approach. The R package *rgl* (Adler  
186 and Murdoch 2016) was used to represent the first three axes of both the PCoA and DFA in  
187 3D scatter plots with 95% confidence ellipses of concentration for the eight taxa.  
188 Distributions of quantitative characters were summarised in the form of beanplots using the R  
189 package *beanplot* (Kampstra 2008). To evaluate the impact of sample size on the results, we  
190 repeated the PCoA and DFA analyses replacing the missing data with mean values, without  
191 obtaining significantly different results. We used the basic packages of R v3.2.5 (R  
192 Development Core Team 2016), *ape* (Paradis et al. 2004) and *vegan* (Oksanen et al. 2011) to  
193 construct the PCoA and *MASS* (Venables and Ripley 2002) for the DFA.

194

195 *Phylogenomic Analysis*

196           *Specimen sampling and DNA extraction.*—We sampled a total of 89 individuals of  
197 *Linaria*. Of these, 76 individuals represented the distribution and morphological variation of  
198 all species and subspecies of the Iberian clade of *Linaria* subsect. *Versicolores*, including  
199 specimens of the two flower colour morphs of SAL and one individual of CRA (Tables 1, S2;  
200 Fig. S1b). Thirteen individuals of additional species of *Linaria* sect. *Versicolores* were  
201 sampled to be used as the outgroup, including the two species of *Linaria* subsect. *Elegantes*  
202 and six species of the North African clade of *Linaria* subsect. *Versicolores* (Tables 1, S2).  
203 Seventy-five individuals were sampled in the field and dried in silica gel between 2006 and  
204 2015, while 14 individuals were obtained from generally older (1970-2006) herbarium  
205 specimens (MA, RNG). For each sampled individual, total genomic DNA was extracted from  
206 c. 20 mg of leaf tissue using a modified CTAB protocol (Doyle and Doyle 1987; Cullings  
207 1992). DNA concentrations were quantified using a Qubit 2.0 fluorometer (Invitrogen, CA,  
208 USA) with the dsDNA Broad-Range Assay Kit.

209  
210           *Genotyping-by-sequencing library preparation.*—A GBS library was prepared using  
211 all DNA samples with the *Pst*I-HF restriction enzyme and following previously published  
212 procedures (Elshire et al. 2011; Escudero et al. 2014; Grabowski et al. 2014) with some  
213 modifications. A full description of laboratory protocols is found in Online Appendix 2, and a  
214 summary is provided here. For each sample, 500 ng (where available) of genomic DNA were  
215 combined with 0.6 pmol of a sample specific barcode adapter and 0.6 pmol of common  
216 adapter (Tables S2, S3). Each sample was digested with 4 units of *Pst*I-HF (NEB, MA, USA)  
217 at 37°C overnight. Adapters were ligated using 400 units of T4 DNA Ligase (NEB, MA,  
218 USA) at room temperature for 4 h. 50 ng of each sample were combined, and the pool was  
219 then purified with Agencourt AMPure XP (Beckman Coulter, CA, USA). DNA fragments  
220 were amplified for 15 PCR cycles starting from 35 ng of DNA and using NEB 2x Taq

221 MasterMix (NEB, MA, USA). The PCR product was purified using different volume ratios of  
222 AMPure XP beads to sample, and fragment size distributions were assessed in a 2100  
223 Bioanalyzer (Agilent Technologies, CA, USA; Fig. S2). The library with the optimal profile  
224 and concentration (AMPure to sample ratio 0.8:1, concentration 1.87 ng/μl, average size 595  
225 bp) was submitted to BGI-Europe (Copenhagen, Denmark) for 100 bp HiSeq 2000 Illumina  
226 sequencing. Quality control of sequencing results was conducted in FastQC 0.11.3 (Andrews  
227 2010).

228

229 *Data assembly and genetic structure.*—Assembly of GBS loci was performed using  
230 the pyRAD 3.0.61 pipeline (Eaton 2014). The pyRAD procedure consisted of seven  
231 sequential steps, with parameters based on those recommended for single-end GBS data in  
232 the pyRAD documentation (<http://dereneaton.com/software/pyrad/>; see Online Appendix 2  
233 for details). Since phylogenetic results are known to be sensitive to the similarity threshold  
234 employed for within-sample and across-sample sequence clustering (c) (Takahashi et al.  
235 2014; Mastretta-Yanes et al. 2015; Shafer et al. 2016), 16 assemblies of GBS loci were  
236 generated using a range of clustering thresholds from c=0.80 to c=0.95. Statistical base  
237 calling was conducted following Li et al. (2008), with a minimum depth of coverage of 6 and  
238 a maximum of 5 Ns in consensus sequences. Filtering of putative paralogs was performed by  
239 setting a maximum of two alleles (corresponding to diploid organisms) and 8 heterozygous  
240 sites per consensus sequence. Loci with a minimum taxon coverage (m, minimum number of  
241 samples with data) of 4 and a maximum of 3 individuals with shared polymorphic sites (as a  
242 further filter of putative paralogs) were retained. Additional assemblies were generated for  
243 particular downstream analyses by excluding specific individuals and varying the minimum  
244 taxon coverage (m=10, m=20; see below). Henceforth, assemblies are denoted as cXmY,  
245 with X being the clustering threshold and Y being the minimum taxon coverage (Table 2).

246 Before starting phylogenetic analyses, we tested the correspondence between  
247 morphologically defined taxa and genetic clusters by analysing unlinked single nucleotide  
248 polymorphism (SNP) matrices using three approaches: principal component analysis (PCA;  
249 Waterhouse et al. 2009), Neighbour-Net phylogenetic network estimation (Bryant and  
250 Moulton 2004) and Bayesian clustering (Pritchard et al. 2000; Corander et al. 2004) (see  
251 Online Appendix 2 for details). As a result of these analyses, eight individuals of uncertain  
252 genetic identity, either because of their putative recent hybrid origin or low-quality  
253 sequencing results (>99% missing data in the final datasets) were excluded from downstream  
254 phylogenetic analyses.

255

256 *Concatenation-based phylogenies.*—Maximum likelihood (ML) analyses of the 16  
257 full-sequence concatenated datasets obtained under 16 clustering threshold values were  
258 implemented in RAxML 8.2.8 (Stamatakis 2014) using the GTRCAT substitution model  
259 (Stamatakis 2006) during tree search, followed by evaluation and optimisation of the final  
260 tree under GTRGAMMA. The four *Linaria* subsect. *Elegantes* samples were set as the  
261 outgroup.

262 Four alternative species-level topologies were found among the 16 ML trees (see  
263 Results). We selected four datasets, each yielding a distinct topology with high bootstrap  
264 support (BS) values, for further analysis and testing: c84m4, c85m4, c87m4 and c92m4. For  
265 these datasets, we additionally explored the performance of ML analyses based on  
266 concatenated SNP matrices (i.e. excluding invariant sites) using two acquisition bias  
267 corrections (Leaché et al. 2015a) implemented in RAxML (see Online Appendix 2 for  
268 details). The four full-sequence matrices were also analysed using Bayesian inference (BI), as  
269 implemented in ExaBayes 1.4.1 (Aberer et al. 2014), with the GTRGAMMA substitution  
270 model. To assess the sensitivity of the results to the minimum taxon coverage, assemblies

271 generated with  $m=10$  and  $m=20$  and the same clustering threshold values (see Table 2) were  
272 analyzed by ML in RAxML using the same methods described above.

273

274 *Coalescent-based phylogenies.*—It is known that the concatenated approach may  
275 produce spurious phylogenetic results, particularly under high ILS, expected in rapid  
276 radiations. Amongst available gene-tree-based methods accounting for ILS, we selected NJ<sub>st</sub>  
277 (Liu and Yu 2011) because of the following features: it is able to infer the species tree from  
278 unrooted gene trees (outgroup samples would be absent from many gene trees in our dataset,  
279 impeding the rooting of gene trees); it can accommodate missing data; and it can handle  
280 allele data from multiple individuals per species. The four selected datasets yielding  
281 contrasting topologies in concatenated analyses (c84m4, c85m4, c87m4 and c92m4) were  
282 separately analysed as follows. For all loci showing variability, gene trees were estimated  
283 using RAxML with the GTR+GAMMA substitution model and 100 bootstrap replicates.  
284 Fifty multilocus bootstrap replicates (Seo 2008; Mallo 2015) were generated, thus resampling  
285 nucleotides within loci, as well as loci within the dataset. The NJ<sub>st</sub> method was implemented  
286 on the fifty bootstrapped matrices using the R script NJstM (Mallo 2016), which relies on the  
287 *phybase* package (Liu and Yu 2010). A 50% majority-rule (MR) consensus tree was then  
288 built from the 50 bootstrap replicates in PAUP\* 4 (Swofford 2002). Additionally, assemblies  
289 generated with higher values of  $m$  ( $m=10$  and  $m=20$ ) and the same clustering threshold  
290 values (see Table 2) were analysed using the same methods described above, to assess the  
291 sensitivity of the results to the minimum taxon coverage.

292 For the same datasets analysed in NJ<sub>st</sub>, we additionally implemented the quartet-based  
293 method SVDquartets (Chifman and Kubatko 2014), also accounting for ILS. This method can  
294 handle both unlinked SNP and multi-locus full-sequence datasets. Therefore, we analysed  
295 both types of matrices generated under the same four clustering threshold values and three

296 minimum taxon coverage values. Analyses were run in PAUP\* 4 under the multispecies  
297 coalescent, evaluating all possible quartets. For each matrix, one hundred bootstrap replicates  
298 were conducted, and results were summarised in a 50% MR consensus tree.

299

300 *Tests of alternative topologies.*—To examine if alternative tree topologies could be  
301 statistically rejected by each of the four selected concatenated datasets (c84m4, c85m4,  
302 c87m4 and c92m4), topology tests were conducted. First, for each of the four sequence  
303 matrices, constrained ML analyses were conducted in RAxML using the four alternative  
304 species-level topologies encountered in unconstrained analyses (topologies 1-4), the  
305 topologies obtained from coalescent-based NJ<sub>st</sub> (topology 5) and SVDquartets (topology 6)  
306 analyses and two additional topologies recovered from previous concatenated (topology 7;  
307 Vigalondo et al. 2015) and coalescent-based (topology 8; Fernández-Mazuecos et al. 2013a)  
308 analyses of ITS+ptDNA sequences. For each matrix, per-site log likelihoods using all  
309 constrained ML topologies were computed in RAxML under the GTR+GAMMA model, re-  
310 estimating model parameters for each tree. Then we used CONSEL v0.20 (Shimodaira and  
311 Hasegawa 2001) to calculate the *p*-values of topology tests, including the approximately  
312 unbiased (AU) test (Shimodaira 2002), the Shimodaira-Hasegawa (SH) test (Shimodaira and  
313 Hasegawa 1999) and the weighted Shimodaira-Hasegawa (WSH) test (Buckley et al. 2001).

314 To visualise differences in the numbers of loci supporting alternative topologies, we  
315 used the “partitioned RAD” approach (Hipp et al. 2014) implemented in the R package  
316 *RADami* (Hipp 2014). The numbers of loci supporting and disfavouring each of the eight  
317 constrained topologies generated for topology tests (see above) were compared for each of  
318 the four selected datasets. A set of unique trees was generated for each locus (by pruning the  
319 original eight trees to those tips present in each locus), and the log likelihood of each unique  
320 tree for each locus was calculated in RAxML under the GTR+GAMMA model. For each

321 locus, trees were then ranked as supported if they were within 2 log likelihood units of the  
322 best supported tree for that locus, or disfavoured if they were within 2 log likelihood units of  
323 the least supported tree for that locus. Finally, for each dataset, the number of loci supporting  
324 or disfavoured each of the eight alternative trees was plotted against the tree log likelihood  
325 calculated using the concatenated matrix.

326

327 *Hybridisation analyses.*—Coalescent-based species tree analyses provided two  
328 alternative topologies (see Results). We explored ancestral hybridisation as a potential source  
329 of these conflicting results using two approaches: *D*-statistic tests (Durand et al. 2011; Eaton  
330 et al. 2015) and the pseudolikelihood-based phylogenetic network method SNaQ (Species  
331 Networks applying Quartets), which incorporates both incomplete lineage sorting and  
332 hybridisation, and employs unrooted gene trees (Solís-Lemus and Ané 2016).

333 Four-taxon *D*-statistic tests (ABBA-BABA tests) were conducted in pyRAD,  
334 including heterozygous sites (Durand et al. 2011; Eaton et al. 2015). Analyses were  
335 performed on the c84m4, c85m4, c87m4 and c92m4 datasets using a set of selected  
336 individuals with good-quality sequencing, and assuming either the NJ<sub>st</sub> or the SVDquartets  
337 phylogeny as the species tree (representing the major vertical inheritance pattern, MVIP). For  
338 each dataset, three sets of tests were conducted exploring the potential role of hybridisation  
339 on the alternative positions of CLE and SPA in the NJ<sub>st</sub>, SVDquartets and concatenation-  
340 based trees (see Online Appendix 2 for details).

341 The SNaQ method (Solís-Lemus and Ané 2016) was implemented using a small set of  
342 27 individuals to reduce computational demand. For each of the c84m4, c85m4, c87m4 and  
343 c92m4 assemblies, ML gene trees were generated in RAxML and used as input for SNaQ  
344 analyses in PhyloNetworks 0.5.0. Since preliminary searches for an optimal network  
345 produced highly inconsistent results in independent runs, we focused on evaluating each of

346 the NJ<sub>st</sub> and SVDquartets species trees as fixed candidate topologies representing the MVIP,  
347 both without reticulation and with reticulation events (hybrid edges) accounting for  
348 incongruences with the alternative species tree topology. After optimisation, the fit of trees  
349 and networks to the data was evaluated based on pseudo-deviance values, and estimated  
350 inheritance probabilities (i.e. the proportion of genes contributed by each parental population  
351 to a hybrid taxon) were visualised.

352

### 353 *Patterns of Morphological Evolution*

354 Morphometric and phylogenomic data were integrated to investigate patterns of  
355 morphological evolution during the radiation of the study clade. A phylomorphospace  
356 approach, implemented in the R package *phytools* (Revell 2012), was used to map the history  
357 of morphological diversification and explore the magnitude and direction of morphological  
358 changes (Sidlauskas 2008). The coalescent-based MR phylogenies obtained in NJ<sub>st</sub> and  
359 SVDquartets, which provided the most robust phylogenetic hypotheses (see below), were  
360 used. After estimating branch lengths by ML (see Online Appendix 2 for details), both trees  
361 were projected onto the multivariate morphospace defined by the first three canonical  
362 discriminant functions of our DFA of vegetative and reproductive traits, with each taxon  
363 represented by the mean values of the functions for all examined individuals. The same  
364 approach was used to project the phylogeny into the two-dimensional flower morphospace  
365 defined by the geometric morphometric study of Fernández-Mazuecos et al. (2013a), based  
366 on canonical variate (CV) analysis of landmark data. For comparison with geographic  
367 patterns of speciation, the phylogeny was also mapped onto the geographic distribution of the  
368 eight taxa in the Iberian Peninsula.

369 In addition, we investigated shifts in particular morphological characters and  
370 instances of phenotypic convergence by conducting ancestral state reconstructions (ASRs) in

371 Mesquite 3.04 (Maddison and Maddison 2011) using the coalescent-based species trees (NJ<sub>st</sub>  
372 and SVDquartets). Maximum parsimony (MP) and ML methods were applied. Four key traits  
373 determining morphological diversity in the study clade were analysed: habit (annual vs.  
374 perennial), inflorescence density (lax vs. dense), dominant corolla colour (purple vs. yellow)  
375 and corolla shape. For corolla shape, three types based on geometric morphometric analyses  
376 were defined (Fernández-Mazuecos et al. 2013a): type I (broad corolla tube and long nectar  
377 spur), type II (broad corolla tube and short nectar spur) and type III (narrow corolla tube and  
378 long nectar spur).

379

## 380 RESULTS

### 381 *Morphometric Analysis*

382 Morphometric analyses revealed the eight taxa in the Iberian clade of *Linaria* subsect.  
383 *Versicolores* as morphologically distinct units (Figs. 1a, b, S3; Table S4). Beanplots (Fig. S3)  
384 depicted differences between taxa in particular morphological traits, especially between CLE  
385 and other taxa for stem length, flower pedicel length, spur width, and corolla/spur length  
386 ratio. The first three coordinates of the PCoA (explaining 54.8% of variance) depicted a  
387 complex morphospace (Fig. 1a), with morphological affinities between individuals and taxa  
388 consistent with taxonomic expectations, and different degrees of morphological variation  
389 within taxa. VIS, SPA and SAL displayed the highest overall morphological variation, while  
390 BEC, CLE and ALG displayed the smallest variation. Individuals of different species did not  
391 generally intermingle in the morphospace, despite some overlap of 95% confidence ellipses  
392 of concentration. CRA specimens were found to fall within the variation of SPA and were  
393 considered as SPA for the DFA analysis.

394 The first three canonical discriminant functions of the DFA (explaining 79.5% of  
395 variation among groups) clearly discriminated CLE from two other clusters of species, one

396 formed by INC and ONU, and the other formed by ALG, BEC, SPA, SAL and VIS (Fig. 1b;  
397 Table S5). The isolation of CLE was mainly the result of significant differences in the ratio  
398 corolla/spur length (Table S5; Fig. S3). In the DFA, 100% of cases were correctly classified  
399 in the original species grouping, and 96.98% in the cross-validated cases, with ALG, BEC  
400 and CLE showing 100% of correct classification (Table S6).

401

## 402 *Phylogenomic Analysis*

403 *Data assembly and genetic structure.*—Illumina sequencing provided c. 155 million  
404 raw reads, with a GC content of 43.05% and bases with quality >Q20 at 96.36%. Assessment  
405 in FastQC showed high quality throughout the full 100 bp length of the first reads and little  
406 signs of contamination (based on per sequence GC content). Assembly in pyRAD with a  
407 minimum taxon coverage of 4 and the full set of individuals resulted in a total number of loci  
408 between 21,283 and 36,435 and a concatenated length of 1.97-3.30 Mbp depending on the  
409 clustering threshold. Percentages of missing data were high (86.41 to 88.85%). The number  
410 of loci, concatenated length and percentage of missing data increased with the clustering  
411 threshold, while the number of parsimony-informative characters (PICs) decreased (Table 2).  
412 The steep increase in number of loci for the highest values of clustering threshold suggested  
413 “over-splitting”, where orthologous sequences are divided into separate loci (Harvey et al.  
414 2015). The average number of loci per species of the study clade ranged between 2,630 (VIS)  
415 and 4,464 (BEC), and the number of sequenced loci per individual decreased quickly with  
416 sample age (Fig. S4), with four herbarium specimens of VIS older than 25 years producing  
417 low-quality results. After excluding problematic individuals, similar numbers of loci and  
418 percentages of missing data were found when using a minimum taxon coverage of 4. When  
419 increasing the minimum taxon coverage, the percentage of missing data improved, but the  
420 number of loci, concatenated length and number of PICs decreased dramatically (Table 2).

421 SNP-based genetic structure analyses produced qualitatively similar results across  
422 datasets. Genetic clusters broadly corresponding with morphologically defined taxa were  
423 recovered by PCA (Fig. 1c), Neighbour-Net (Fig. S5a) and Bayesian clustering (Fig. S5b)  
424 analyses. The CRA individual was consistently included in the SPA cluster. Individuals of  
425 the two colour morphs of SAL were consistently included in the same genetic cluster. Eight  
426 individuals with uncertain genetic affinities were excluded from further analyses, including  
427 six individuals of VIS, one of SPA and one of ONU (see Online Appendix 2 for details).

428

429 *Concatenation-based phylogenies.*—ML phylogenetic analyses of the 16 datasets  
430 supported the monophyly of the Iberian clade of *Linaria* subsect. *Versicolores* and its sister  
431 relationship to the North African clade (Figs. 2a-d, S6). The eight taxa were recovered as  
432 monophyletic groups with 100% BS, and four alternative species-level topologies were  
433 obtained (Figs. 2a-d, 3). Three pairs of sister species were consistently recovered from all  
434 datasets: (BEC,SAL), (VIS,ONU) and (SPA,INC). In contrast, two species displayed two  
435 alternative phylogenetic placements each with variable BS: CLE was recovered as either  
436 sister to a clade formed by the remaining 7 species (8 datasets, e.g. Fig. 2c, d) or sister to the  
437 (BEC,SAL) clade (8 datasets, e.g. Fig. 2a, b); and ALG was recovered as either sister to a  
438 ((VIS,ONU),(SPA,INC)) clade (10 datasets, e.g. Fig. 2a, d) or sister to the (SPA,INC) clade  
439 (6 datasets, e.g. Fig. 2b, c). The c84m4, c85m4, c87m4 and c92m4 datasets were selected as  
440 representatives of the four alternative topologies (topologies 1-4) for further analysis because  
441 of their high average BS for species-level divergences. Topologies produced by ML analyses  
442 of concatenated SNP matrices fell within the range of topologies produced by full-sequence  
443 analyses (Fig. S7; see Online Appendix 2 for details).

444 BI phylogenetic analyses of the c84m4, c85m4, c87m4 and c92m4 datasets recovered  
445 MR trees topologically identical to the ML trees obtained from the same datasets, and

446 displaying high posterior probabilities ( $PP \approx 1$ ) for all species divergences (Fig. 2a-d). When  
447 increasing the minimum taxon coverage parameter, ML analyses (Fig. S6) displayed varied  
448 topologies with a general decrease in statistical support of clades (particularly for  $m=20$ ).

449

450 *Coalescent-based phylogenies.*—Unlike the contrasting topologies obtained from  
451 concatenated analyses, coalescent-based  $NJ_{st}$  analyses of the c84m4, c85m4, c87m4 and  
452 c92m4 datasets produced identical MR topologies, although with variable BS values (Figs.  
453 2e, S8). The monophyly of the Iberian clade of *Linaria* subsect. *Versicolores* (98-100% BS)  
454 and its sister relationship to the North African clade were strongly supported. Two major,  
455 geographically structured subclades were recovered within the Iberian clade (Figs. 2e, 4a, 5):  
456 a clade formed by SAL, BEC and CLE, endemic to the south-eastern Iberian Peninsula (74-  
457 94% BS); and a clade formed by VIS, ONU, ALG, SPA and INC, mostly distributed in the  
458 western Iberian Peninsula (100% BS in all analyses). Within the south-eastern Iberian clade,  
459 SAL was recovered as sister to a (BEC,CLE) clade. This phylogenetic position of CLE as  
460 sister to BEC (94-100% BS) was not recovered from concatenated analyses. Within the  
461 western Iberian clade, two sister species pairs found in the  $NJ_{st}$  tree were also consistently  
462 recovered from concatenated analyses: (VIS,ONU) (100% BS in all analyses) and (SPA,INC)  
463 (88-100% BS). ALG was recovered as sister to the (SPA,INC) pair, one of the two alternative  
464 positions identified in concatenated analyses. When increasing the minimum taxon coverage  
465 parameter to  $m=10$ , we obtained the same MR topology for all datasets, although with lower  
466 BS values. For  $m=20$ , there was a general loss of resolution, including basal polytomies and  
467 poor BS values (Fig. S8).

468 SVDquartets analyses produced another topology (Figs. 2f, S8) that was highly robust  
469 to variations in clustering threshold and minimum taxon coverage. The monophyly of the  
470 Iberian clade (98-100% BS for analyses with  $m=4$ ) and its sister relationship to the North

471 African clade were again strongly supported, but there were two differences with the NJ<sub>st</sub>  
472 tree: CLE was consistently recovered as sister to a clade formed by the remaining seven  
473 species (100% BS), and SPA was found to form a clade (69-97% BS) with the (VIS,ONU)  
474 pair (75-88% BS). The same topology was obtained for all analyses with m=10 and three out  
475 of four analyses with m=20 (Fig. S8).

476

477 *Tests of alternative topologies.*—The two topologies obtained in previous analyses of  
478 ITS+ptDNA sequences (topologies 7, 8) were strongly rejected by all tests implemented for  
479 all analysed GBS datasets (Table 3). The SVDquartets tree (topology 6) was rejected by all  
480 tests for the c85m4, c87m4 and c92m4 datasets. None of the remaining five topologies (four  
481 concatenated and NJ<sub>st</sub>) were consistently rejected. SH tests could not reject any of these five  
482 topologies for any of the datasets, while WSH tests only rejected the NJ<sub>st</sub> topology (topology  
483 5) for the c92m4 dataset. AU tests rejected the NJ<sub>st</sub> topology for the c87m4 and c92m4  
484 datasets and one of the concatenation-based topologies (topology 2) for the c92m4 dataset.  
485 All remaining *p*-values were non-significant (Table 3).

486 Topologies 7 and 8 were also consistently supported by the smallest numbers of loci  
487 and disfavoured by the highest numbers of loci (Fig. 3). The ML tree for each concatenated  
488 dataset was also supported by the highest number and disfavoured by the smallest number of  
489 loci. The remaining coalescent- and concatenation-based topologies were supported and  
490 disfavoured by intermediate numbers of loci, with the NJ<sub>st</sub> tree being consistently supported  
491 by more loci than the SVDquartets tree (Fig. 3).

492

493 *Hybridisation analyses.*—When assuming the NJ<sub>st</sub> species tree as MVIP in *D*-statistic  
494 tests, we found clear evidence for an excess of shared derived alleles between BEC and SAL  
495 in three of the datasets (24-30% of significant tests depending on the dataset) but weaker

496 evidence for an excess of shared derived alleles between SPA and VIS/ONU (8-13% of  
497 significant tests) (Table 4). When assuming the SVDquartets species tree as MVIP, the tests  
498 (Table 4) found evidence for an excess of shared derived alleles between SPA and INC (24-  
499 41% of significant tests), and between BEC and CLE (18-35% of significant tests).

500 Evaluation of the NJ<sub>st</sub> and SVDquartets trees without reticulations in SNaQ (Table 5,  
501 Fig. 2g, h) consistently supported the NJ<sub>st</sub> tree for all analysed datasets. When including  
502 reticulations accounting for incongruences between species tree topologies, three datasets  
503 (c85m4, c87m4, c92m4) supported the NJ<sub>st</sub> topology as MVIP, while the c84m4 dataset  
504 supported the SVDquartets topology (although in this case with a small difference in pseudo-  
505 deviance values). For the best supported network (with the NJ<sub>st</sub> tree as MVIP), CLE was  
506 estimated to contain a 81-85% genomic contribution from a lineage sister to BEC and 15-  
507 19% from an ancestral lineage sister to the other seven species of the clade. Similarly, SPA  
508 was estimated to contain a 81-87% contribution from a lineage sister to INC and a 13-19%  
509 contribution from a lineage sister to the (VIS,ONU) clade.

510

511

### 512 *Patterns of Morphological Evolution*

513 The phylomorphospace based on vegetative and reproductive traits and the NJ<sub>st</sub>  
514 species tree (Fig. 4b) suggested that SAL has retained morphological traits close to those of  
515 the common ancestor of the Iberian clade, while other species have experienced extensive  
516 morphological change in multiple directions. Changes of great magnitude in opposite  
517 directions of the morphospace are inferred during the divergence of pairs of sister species,  
518 including BEC/CLE, VIS/ONU and, to a lesser extent, SPA/INC. At the same time,  
519 convergence is suggested by the proximity in the morphospace of non-closely related species  
520 pairs, such as INC/ONU, BEC/ALG and SAL/SPA. When focusing on flower shape (Fig.

521 4c), morphological disparity between sister species was even more striking. The ancestral  
522 flower for the clade seems to have had a corolla with a broad tube and relatively long nectar  
523 spur (type I), a basic shape that has been retained by five species in both subclades (SAL,  
524 BEC, SPA, VIS and ALG). Speciation in the sister species pairs VIS/ONU and SPA/INC  
525 involved extensive change in flower shape along CV1, which independently gave rise to  
526 narrow-tubed, long-spurred flowers (Type III) in ONU and INC. By contrast, speciation of  
527 the BEC/CLE pair involved extensive change along CV2, producing the short-spurred, broad-  
528 tubed flowers (type II) of CLE. The longest-spurred type I flowers (with the lowest values of  
529 CV2) have evolved independently in BEC (sister to CLE) and ALG. Mapping of the  
530 phylogeny onto geographic ranges showed that pairs of morphologically divergent sister  
531 species display geographically close or even overlapping distributions (Fig. 5): BEC and CLE  
532 are both narrow endemics to the same small region in south-eastern Spain; VIS and ONU  
533 occur in south-western Iberia; and the distributions of SPA and INC largely overlap in the  
534 central-western Peninsula. MP reconstructions based on the  $NJ_{st}$  tree (Fig. S9a)  
535 unambiguously inferred a single shift from annual to perennial habit (in CLE), and multiple  
536 shifts in inflorescence habit, dominant corolla colour and corolla shape. ML reconstructions  
537 (Fig. S9b) produced similar results.

538 Broadly similar patterns of morphological evolution were inferred from the  
539 SVDquartets tree (Fig. S9c-f), including extensive morphological change associated with  
540 speciation events, as well as phenotypic convergence. In phylomorphospace analyses, the  
541 main differences resulted from the early-diverging position of CLE in this tree. As a  
542 consequence, the extensive morphological change leading to CLE was associated with the  
543 first speciation event in the Iberian clade, instead of a more recent divergence with BEC.

544

545 DISCUSSION

547 Our genotyping-by-sequencing approach proved successful in generating highly  
548 informative genome-wide genetic markers, not only across the recent (Quaternary) radiation  
549 of our 8-species study clade, but also across the whole *Linaria* sect. *Versicolores*, whose most  
550 recent common ancestor has been dated back to the late Miocene-Pliocene (Fernández-  
551 Mazuecos and Vargas 2011; Fernández-Mazuecos et al. 2013a). Regardless of the method  
552 used for phylogenetic inference, inferred basal relationships (i.e. the monophyly and sister  
553 relationship of the Iberian and North African clades of subsect. *Versicolores*; Figs. 2, 4a)  
554 were identical to those obtained using conventional phylogenetic markers. The two major  
555 subclades within the Iberian clade supported by coalescent-based analyses of GBS data in  
556 NJ<sub>st</sub> (Fig. 4a) broadly corresponded to those already obtained (with varying support) in a  
557 coalescent-based analysis of ITS and ptDNA sequences and in a concatenated analysis of  
558 ptDNA sequences (but they were inconsistent with those obtained using ITS sequences alone)  
559 (Fernández-Mazuecos et al. 2013a; Fernández-Mazuecos and Vargas 2015). However, apart  
560 from major subclades, previous species-level topologies found little support in our genome-  
561 wide data, and comparatively more reliable phylogenetic hypotheses were inferred herein. In  
562 addition, genetic structure analyses recovered unprecedented resolution of species  
563 boundaries, as shown by the congruence between inferred genetic clusters and  
564 morphologically-defined species (Figs. 1, S5).

565 Therefore, despite the uncertainties remaining (possibly explained by hybridisation;  
566 see below), our results show that GBS can provide unprecedented systematic and  
567 phylogenetic resolution in recent radiations where conventional markers failed, and without  
568 the need for previous genomic information (Escudero et al. 2014). Given their relatively  
569 simple and inexpensive implementation, GBS and similar methods of the GBS/RAD-Seq  
570 family may be universally and routinely applicable by systematic biologists as a NGS-based

571 replacement to conventional phylogenetic approaches (Ree and Hipp 2015; de la Harpe et al.  
572 2017; Hamon et al. 2017). Indeed, after DNA extraction, GBS library preparation can be  
573 carried out in 2-3 days using equipment available in most molecular systematic laboratories,  
574 and successful results may be obtained by multiplexing c.100 individuals in a single HiSeq  
575 Illumina lane (although the allowed level of multiplexing would depend on genome sizes and  
576 GC content as well as number of reads per lane). Interestingly, even though recently collected  
577 tissue is clearly preferable due to a decline in sequencing success with sample age as a result  
578 of DNA degradation, we still obtained >1000 sequenced loci with herbarium samples as old  
579 as 20-30 years (Fig. S4; but see an improved method for highly degraded DNA samples in  
580 Suchan et al. 2016). Compared to the RAD-Seq procedure (Baird et al. 2008), which has been  
581 more widely used in phylogenetic and population genetic studies in recent years, the GBS  
582 protocol of Elshire et al. (2011) has the advantage of a much simpler protocol for library  
583 preparation, including fewer purification steps (thus increasing the probability of success with  
584 low starting amounts) and of not requiring accurate size selection of DNA fragments  
585 (therefore involving less specialised equipment).

586         The main drawback of GBS, particularly when applied to phylogenetics, is the high  
587 proportion of missing data in the assembled datasets (Table 2). This problem is shared by  
588 RAD-Seq, although to a lesser extent thanks to size selection. Datasets with lower  
589 percentages of missing data may be obtained by increasing the minimum taxon coverage,  
590 therefore restricting the final dataset to those loci that were sequenced in a high percentage of  
591 individuals. Still, simulations show that accurate phylogenies can be obtained from datasets  
592 including vast amounts of missing data (Rubin et al. 2012). Furthermore, increasing the  
593 minimum taxon coverage may result in the loss of valuable phylogenetic information due to  
594 reduced dataset size and a biased representation of the mutation spectrum across sequenced  
595 loci (Huang and Knowles 2014). This is consistent with our empirical results, in which the

596 numbers of loci dramatically decreased when increasing the minimum taxon coverage (Table  
597 2), resulting in a loss of phylogenetic resolution in both concatenated and coalescent-based  
598 analyses (Fig. S6, S8). Nevertheless, more complete GBS datasets may be obtained, at the  
599 same time preventing information loss, by multiplexing smaller numbers of samples per  
600 Illumina lane (thus increasing sequencing coverage) and optimising the quality of starting  
601 DNA.

602

### 603 *Concatenation vs. Coalescent-based Approaches to GBS Phylogenetics*

604 A concatenation approach has been widely used for the analysis of restriction digest-  
605 based phylogenomic datasets (e.g. Nadeau et al. 2013; Wagner et al. 2013; Escudero et al.  
606 2014; Hipp et al. 2014; Cavender-Bares et al. 2015). In particular, ML in RAxML is the  
607 current standard for concatenated analysis thanks to its high efficiency with large data  
608 matrices. However, there are several well-known drawbacks of concatenated analysis  
609 (Wagner et al. 2013). Concatenation assumes a shared phylogenetic history for all sequenced  
610 genes, and therefore it is inconsistent in the presence of gene tree discordance caused by ILS  
611 and hybridisation (Kubatko and Degnan 2007; Solís-Lemus et al. 2016). Accuracy of species  
612 phylogenies inferred by concatenation relies on the most frequent gene tree topology being  
613 the same as the species tree topology, but “anomaly zones” exist under certain conditions  
614 (involving short branch lengths) in which the most likely gene tree topology differs from the  
615 species tree (Degnan and Rosenberg 2006). Additionally, as phylogenomic datasets grow  
616 larger, concatenation is more likely to produce anomalously high statistical support for  
617 incorrect topologies as a result of systematic biases (Gadagkar et al. 2005; Kumar et al.  
618 2011). Bias may result from the specification of a single substitution model, which assumes  
619 substitution rate homogeneity across the whole dataset. Partitioned analysis may prevent this  
620 problem, but it may be computationally problematic with high numbers of loci. Issues with

621 orthology determination and alignment can also result in biases (Kumar et al. 2011), which  
622 may be alleviated if a sequenced genome is available as reference for data assembly. Finally,  
623 another well-known cause of bias is long-branch attraction, which may be mitigated by a  
624 complete taxonomic sampling and by avoiding those methods that are more sensitive to it,  
625 such as parsimony (Bergsten 2005).

626         Analyses of our GBS datasets highlight such shortcomings of concatenation. The high  
627 statistical support, as measured by both ML bootstrap and Bayesian posterior probabilities,  
628 for alternative topologies (Fig. 2a-d) is a sign of systematic bias (Kumar et al. 2011) resulting  
629 from the different clustering thresholds. This is true for both concatenated full-sequence and  
630 SNP matrices (Figs. S6, S7). Indeed, changes in the clustering threshold produce contrasting  
631 optimal topologies (with alternative phylogenetic positions for two species) as a result of  
632 significant changes in the numbers of loci supporting and disfavoured alternative trees (Fig.  
633 3). Interestingly, in contrast to the misleading confidence suggested by BS and PP values,  
634 topology tests revealed no such certainty, as they were generally unable to reject topologies  
635 produced by alternative GBS datasets (they did reject previously-published topologies based  
636 on only two loci; Table 3). This bias potentially introduced during data assembly at the  
637 crucial steps of orthology determination casts doubts on any concatenation analysis based on  
638 a fixed clustering threshold. While methods have been proposed to optimise clustering  
639 parameters (Mastretta-Yanes et al. 2015), the significant topological changes that we found  
640 associated with small changes in the clustering threshold (as small as 1%; Fig. 2a-d) indicate  
641 that multiple analyses based on a range of values (Takahashi et al. 2014; Leaché et al.  
642 2015b), combined with topology tests, are still necessary to evaluate if high clade support  
643 values provide a realistic measurement of confidence.

644 In contrast to concatenation, gene-tree-based coalescent methods have been less frequently  
645 used for the inference of species trees from restriction digest-based NGS data. The short

646 length of sequenced loci when analysing single-end data (c. 100-200 bp) may result in poorly  
647 informative gene trees based on individual loci, which may be a problem for species tree  
648 inference (Salichos and Rokas 2013; Mirarab et al. 2016), and full probabilistic methods co-  
649 estimating gene trees and species trees (Liu 2008; Heled and Drummond 2010) are generally  
650 unable to handle large NGS datasets (Wagner et al. 2013). Unlike full probabilistic methods,  
651 summary methods that operate by combining previously estimated gene trees (e.g. Liu and  
652 Yu 2011; Mirarab et al. 2014) are computationally efficient with large datasets. Even with  
653 short loci, one of these methods (NJ<sub>st</sub>) allowed us to infer a resolved species tree (Figs. 2e,  
654 4a), showing that the implementation of summary methods is computationally feasible with  
655 GBS and RAD-Seq data (see also Ebel et al. 2015; DaCosta and Sorenson 2016). Moreover,  
656 the same species tree was produced by this coalescent method from datasets assembled using  
657 different clustering thresholds that produced contrasting topologies in concatenation analyses  
658 and, furthermore, the NJ<sub>st</sub> topology could not be rejected by a majority of topology tests using  
659 the concatenated datasets (Table 3). The NJ<sub>st</sub> topology was similar to the concatenation-based  
660 topologies, with one of the problematic species, ALG, consistently recovered at one of the  
661 two alternative positions of the concatenated analyses (although with varying support). By  
662 contrast, the other problematic species, CLE, was recovered as sister to BEC, a relationship  
663 not found in concatenated analyses but biogeographically reasonable, given the close  
664 proximity of the two species' narrow distributions (Fig. 5). All other species remained at the  
665 phylogenetic placements found in concatenation analyses.

666         As an alternative to gene-tree-based methods, coalescent-based approaches that  
667 bypass the inference of gene trees have been proposed (Bryant et al. 2012; Chifman and  
668 Kubatko 2014) and applied to RAD-Seq datasets (DaCosta and Sorenson 2016; Manthey et  
669 al. 2016). We tested the performance of the SVDquartets method, which infers relationships  
670 among quartets of taxa using algebraic statistics (Chifman and Kubatko 2014). While poor

671 resolution and support values were recovered when analysing unlinked SNP matrices (Fig.  
672 S8), analyses of full-sequence matrices produced a well-supported topology that was highly  
673 robust to variations in assembly parameters (Figs. 2f, S8), but different to the NJ<sub>st</sub> topology.  
674 In the SVDquartets tree, CLE was sister to the remaining seven species, a position  
675 encountered in some concatenated analyses. SPA was related to VIS and ONU, a position  
676 only obtained for one concatenated dataset (c84m20; Fig. S6), but consistent with the close  
677 proximity of these tree species in the SNP-based PCA (Fig. 1c).

678         Robustness of phylogenetic patterns across methods and data is considered crucial in  
679 phylogenomics (Kumar et al. 2011). The constancy of the NJ<sub>st</sub> and SVDquartets species trees  
680 across datasets indicates that coalescent analyses may be more robust than concatenation to  
681 systematic bias introduced during dataset assembly. This result adds to the list of advantages  
682 of coalescent methods over concatenation, including their accuracy in the presence of gene  
683 tree discordance caused by ILS (Mirarab et al. 2016) and their more realistic measures of  
684 clade statistical support (Giarla and Esselstyn 2015).

685         The question remains as to the robustness of our results to the violation of the main  
686 assumption of most coalescent methods, i.e. the absence of inter-specific gene flow. Indeed,  
687 historical hybridisation may be behind the contrasting topologies of the NJ<sub>st</sub> and SVDquartets  
688 trees. We minimized the effect of recent hybridisation by excluding individuals suggested as  
689 hybrids by genetic structure analyses. However, *D*-statistic tests (Table 4) still supported  
690 ancestral hybridisation events during diversification of the clade, as indicated by significant  
691 asymmetries in the sharing of derived alleles between non-sister species when using either  
692 tree as the major vertical inheritance pattern. These results show that a fully bifurcating  
693 species tree is an oversimplified representation of the diversification of young clades.  
694 Simulations indicate that coalescent methods, including NJ<sub>st</sub>, are able to infer the correct  
695 dominant species tree in the presence of low levels of gene flow, given a sufficiently large

696 number of genes (Solís-Lemus et al. 2016). With high levels of gene flow, coalescent  
697 methods may not be able to recover the true dominant topology, but they are still more  
698 accurate than concatenation (Solís-Lemus et al. 2016). We propose that both coalescent-  
699 based topologies (and possibly the concatenation-based topologies to an extent) obtained  
700 from our GBS data represent different aspects of a reticulate history of diversification (Fig.  
701 4a). At the same time, we favour the NJ<sub>st</sub> tree over the SVDquartets tree as the current best  
702 estimate of the major pattern of speciation based on the following lines of evidence: (i) the  
703 NJ<sub>st</sub> tree generally fitted the data better in SNaQ analyses, both with and without  
704 hybridisation (Table 5); (ii) the SVDquartets tree was more frequently rejected in topology  
705 tests (Table 3); and (iii) the NJ<sub>st</sub> tree was supported by more gene trees (Fig. 3). In any case,  
706 we cannot minimise the potential role of homoploid hybrid speciation, already suggested for  
707 other *Linaria* clades (Blanco-Pastor et al. 2012; see also Nieto Feliner et al. 2017). The origin  
708 of *L. clementei* is particularly intriguing, as it may have involved hybridisation between an  
709 early-diverging lineage and a recently-derived one (probably with a higher contribution of the  
710 latter according to SNaQ analyses; Table 5; Fig. 2g).

711

### 712 *Phenotypic Divergence and Convergence during Speciation*

713 Our combination of multivariate morphometric, genetic structure and coalescent-  
714 based phylogenetic analyses for the first time provide a well-resolved picture of systematics  
715 and patterns of morphological evolution in a Mediterranean plant lineage, the Iberian clade of  
716 *Linaria* subsect. *Versicolores*. The data support a systematic hypothesis with eight  
717 morphologically and genetically distinct species. Taxonomic notes are provided in Online  
718 Appendix 1. Our results are essentially consistent with previous taxonomic revisions (Sutton  
719 1988; Sáez and Bernal 2009), except that *L. salzmannii* had been generally considered a  
720 subspecies of *L. viscosa* (*L. viscosa* subsp. *spicata*) but is now supported as a distinct species

721 as a result of both taxa being independently derived in all phylogenetic analyses (Figs. 2, 4a;  
722 see also Blanca et al. 2017). A flower colour polymorphism within *L. salzmannii* (Boissier  
723 1841; Sáez and Bernal 2009) is confirmed, as shown by the morphological and genetic  
724 similarity of the yellow- and purple-flowered morphs, and *L. becerrae* is well supported as  
725 distinct from *L. salzmannii* (Blanca et al. 2017). The morphologically similar (particularly in  
726 flower traits) *L. spartea* and *L. viscosa* are established as genetically distinct and non-sister  
727 species (Figs. S5, 2, 4a), although further population genetic sampling would be required to  
728 determine the exact limits of their geographic ranges. Finally, plants collected in the *locus*  
729 *classicus* of *L. viscosa* subsp. *crassifolia* are found to fall within the morphological and  
730 genetic variation of *L. spartea* (Figs. 1, S5, S3).

731 Mapping of morphological traits and geography onto the NJ<sub>st</sub> phylogeny (which we  
732 consider a good estimate of major speciation events) shows a pattern in which closely related  
733 species have geographically close or overlapping distributions, but they are strikingly  
734 divergent in phenotypic traits, and potentially ecological interactions (Figs. 4, 5, S9a, b). At  
735 the same time, unrelated species have evolved convergent phenotypes in different geographic  
736 regions. This pattern has been found in large scale replicated island radiations (Mahler et al.  
737 2013), but is documented here for a smaller scale radiation in a continental setting (see  
738 Hughes and Eastwood 2006; Mittelbach and Schemske 2015). The deeper splits show a  
739 geographic pattern, reflecting the progressive colonization of the Iberian Peninsula during the  
740 Quaternary (Fernández-Mazuecos et al. 2013a; Fernández-Mazuecos and Vargas 2015). The  
741 major phylogenetic split between south-eastern and western species coincides with a  
742 phylogeographic discontinuity found for ptDNA markers (Fernández-Mazuecos and Vargas  
743 2015). There is no clear pattern of morphological differentiation linked to this split, as  
744 indicated by the phylomorphospace based on both vegetative and reproductive characters  
745 (Fig. 4b). In contrast, extensive morphological divergence is associated with recent splits

746 between sister species (Figs. 4b, c, S9a, b). This is particularly true for floral traits related to  
747 pollinator specialisation (Fenster et al. 2004), including corolla colour, corolla shape, nectar  
748 spur length and tube width. Three recent splits between sister species are revealed by the  
749 phylogeny. One of them, in the south-eastern subclade, has led to the divergent flower  
750 morphologies of *L. clementei* and *L. becerrae*, respectively displaying the shortest and one of  
751 the two longest nectar spurs in the clade (Fig. 4). In addition, *L. clementei* is the only  
752 perennial species in the clade, which adds to the singularity of this species (see also DFA  
753 results; Fig. 1b) and its phenotypic divergence with the annual *L. becerrae*. The two other  
754 recent speciation events, in the western subclade, *L. viscosa* – *L. onubensis* in southwestern  
755 Iberia and *L. spartea* – *L. incarnata* in central Iberia, also represent high degrees of  
756 phenotypic divergence. Interestingly, they have both followed nearly identical pathways of  
757 floral change in different geographic regions, including divergence in corolla colour (yellow  
758 in *L. viscosa* and *L. spartea*, and purple-dominated in their sisters *L. onubensis* and *L.*  
759 *incarnata*), corolla tube width (broad in *L. viscosa* and *L. spartea*, narrow in *L. onubensis* and  
760 *L. incarnata*), and overall flower shape (with parallel divergence along the first axis of the  
761 geometric morphometric analysis) (Fig. 4, S9a, b). The most likely floral ancestral  
762 morphology for the western subclade, and for the two pairs of sister species, corresponds to a  
763 purple corolla with broad tube and type I shape. *L. algarviana* is the only species in the  
764 subclade that has retained this ancestral morphology (except for its elongated nectar spur),  
765 while convergent changes have happened in the two other pairs of sister species: a yellow  
766 corolla has independently evolved in *L. spartea* and *L. viscosa* from purple-flowered  
767 ancestors, and a narrow-tubed, type III corolla has independently evolved in *L. onubensis* and  
768 *L. incarnata* from broad-tubed, type I ancestors (Figs. 4, S9a, b). Broad- and narrow-tubed  
769 flowers have been suggested as distinct evolutionary optima representing divergent strategies  
770 of pollen placement on nectar-feeding insects (Fernández-Mazuecos et al. 2013a). Other

771 instances of phenotypic convergence in geographically disjunct species include the additional  
772 shift to a yellow from a purple-dominated corolla in most of the range of *L. salzmännii*, the  
773 independent evolution of dense inflorescences from lax inflorescences in the south-eastern  
774 subclade and *L. viscosa*, and the independent evolution of the longest nectar spurs in *L.*  
775 *becerrae* and *L. algarviana* (Figs. 4, S9a, b).

776         General patterns of morphological evolution are similar when analysing the  
777 SVDquartets tree (Fig. S9c-f). Even though some of the details are different, morphological  
778 divergence between close relatives and convergence between non-close relatives is still  
779 detected, indicating that our main evolutionary inferences are robust to the uncertainty in  
780 topology and to hypothesised reticulation events. Similar results have been obtained,  
781 although with lower resolution, in the North African clade of *Linaria* subsect. *Versicolores*  
782 (Fernández-Mazuecos et al. 2013a) and in *Linaria* sect. *Supinae* (Blanco-Pastor et al. 2015),  
783 pointing to a general pattern in the genus.

784

785         In summary, our results indicate a higher robustness of coalescent approaches, as  
786 compared to concatenation, for GBS-based species phylogenetics. In our study clade,  
787 combined roles of geographical and ecological isolation in speciation are suggested, together  
788 with a likely role of hybridisation. Recent speciation events involve extensive divergence in  
789 key traits linked to pollinator interactions, such as the length of the nectar spur, considered a  
790 key innovation and a model system for eco-evo-devo studies of plant speciation (Fernández-  
791 Mazuecos and Glover 2017). These patterns suggest adaptive, ecological diversification,  
792 including cases of “parallel speciation” likely associated with similar isolating barriers and  
793 selective pressures in different regions.

794

795         FUNDING

796 This work was supported by the Marie Curie Intra-European Fellowship *LINARIA-*  
797 *SPECIATION* (FP7-PEOPLE-2013-IEF, project reference 624396) and an Isaac Newton  
798 Trust Research Grant (Trinity College, Cambridge).

799

#### 800 ACKNOWLEDGEMENTS

801 The authors thank Matthew Dorling for technical assistance; Edwige Moyroud,  
802 Marcial Escudero, José Luis Blanco-Pastor, Irene Villa, Isabel Liberal, Yurena Arjona, Sam  
803 Brockington, Paul Grabowski, Natasha Elina and Cristina Ariani for their support and useful  
804 discussion at different stages of this study; Bruno Santos and Greg Habrych for bioinformatic  
805 assistance; the David Baulcombe lab for permission to use laboratory and bioinformatic  
806 resources; Alberto Fernández-Mazuecos and Joaquín Ramírez for fieldwork support; José  
807 Quiles, Jesús Vílchez, Lucas Gutiérrez, Enrique Sánchez-Gullón, Isabel Marques and Belén  
808 Estébanez for plant materials and/or population locations; the MA, RNG, ABH, SEV, JAEN,  
809 BCB, COI, LISU and SALA herbaria for plant materials; Mats Hjertson, Laurence Loze,  
810 Laurent Gautier and Roxali Bijmoer for their support in solving taxonomic questions; and  
811 three anonymous reviewers for their helpful comments.

812

#### 813 REFERENCES

- 814 Aberer A.J., Kobert K., Stamatakis A. 2014. ExaBayes: massively parallel Bayesian tree  
815 inference for the whole-genome era. *Mol. Biol. Evol.* 31:2553-2556.
- 816 Adler D., Murdoch D. 2016. RGL - 3D real-time visualization device system for R. Available  
817 in <http://rgl.neoscientists.org/>.
- 818 Álvarez I., Wendel J.F. 2003. Ribosomal ITS sequences and plant phylogenetic inference.  
819 *Mol. Phylogenet. Evol.* 29:417-434.

820 Andrews S. 2010. FastQC: a quality control tool for high throughput sequence data.  
821 Available in <http://www.bioinformatics.babraham.ac.uk/projects/fastqc/>.

822 Baird N.A., Etter P.D., Atwood T.S., Currey M.C., Shiver A.L., Lewis Z.A., Selker E.U.,  
823 Cresko W.A., Johnson E.A. 2008. Rapid SNP discovery and genetic mapping using  
824 sequenced RAD markers. PLOS ONE 3:e3376.

825 Bergsten J. 2005. A review of long-branch attraction. Cladistics 21:163-193.

826 Blanca G., Cueto M., Fuentes J. 2017. *Linaria becerrae* (Plantaginaceae), a new endemic  
827 species from the southern Spain, and remarks on what *Linaria salzmannii* is and is  
828 not. Phytotaxa 298:261-268.

829 Blanco-Pastor J.L., Ormosa C., Romero D., Liberal I.M., Gómez J.M., Vargas P. 2015. Bees  
830 explain floral variation in a recent radiation of *Linaria*. J. Evolution. Biol. 28:851-  
831 863.

832 Blanco-Pastor J.L., Vargas P., Pfeil B.E. 2012. Coalescent simulations reveal hybridization  
833 and incomplete lineage sorting in Mediterranean *Linaria*. PLOS ONE 7:e39089.

834 Boissier P.E. 1841. Voyage botanique dans le midi de l'Espagne. Tome II. Paris: Gide et Cie.

835 Bryant D., Bouckaert R., Felsenstein J., Rosenberg N.A., RoyChoudhury A. 2012. Inferring  
836 species trees directly from biallelic genetic markers: bypassing gene trees in a full  
837 coalescent analysis. Mol. Biol. Evol. 29:1917-1932.

838 Bryant D., Moulton V. 2004. Neighbor-net: an agglomerative method for the construction of  
839 phylogenetic networks. Mol. Biol. Evol. 21:255-265.

840 Buckley T.R., Simon C., Shimodaira H., Chambers G.K. 2001. Evaluating hypotheses on the  
841 origin and evolution of the New Zealand alpine cicadas (Maoricicada) using multiple-  
842 comparison tests of tree topology. Mol. Biol. Evol. 18:223-234.

843 Castro M., Castro S., Loureiro J. 2012. Genome size variation and incidence of polyploidy in  
844 Scrophulariaceae sensu lato from the Iberian Peninsula. AoB Plants 2012:pls037.

845 Cavender-Bares J., González-Rodríguez A., Eaton D.A.R., Hipp A.A.L., Beulke A., Manos  
846 P.S. 2015. Phylogeny and biogeography of the American live oaks (*Quercus*  
847 subsection *Virentes*): A genomic and population genetics approach. *Mol. Ecol.*  
848 24:3668-3687.

849 Chifman J., Kubatko L. 2014. Quartet inference from SNP data under the coalescent model.  
850 *Bioinformatics* 30:3317-3324.

851 Corander J., Waldmann P., Marttinen P., Sillanpää M.J. 2004. BAPS 2: enhanced  
852 possibilities for the analysis of genetic population structure. *Bioinformatics* 20:2363-  
853 2369.

854 Cullings K.W. 1992. Design and testing of a plant-specific PCR primer for ecological and  
855 evolutionary studies. *Mol. Ecol.* 1:233-240.

856 DaCosta J.M., Sorenson M.D. 2016. ddRAD-seq phylogenetics based on nucleotide, indel,  
857 and presence-absence polymorphisms: analyses of two avian genera with contrasting  
858 histories. *Mol. Phylogenet. Evol.* 94:122-135.

859 Davey J.W., Hohenlohe P.A., Etter P.D., Boone J.Q., Catchen J.M., Blaxter M.L. 2011.  
860 Genome-wide genetic marker discovery and genotyping using next-generation  
861 sequencing. *Nat. Rev. Genet.* 12:499-510.

862 de la Harpe M., Paris M., Karger D., Rolland J., Kessler M., Salamin N., Lexer C. 2017.  
863 Molecular ecology studies of species radiations: current research gaps, opportunities,  
864 and challenges. *Mol. Ecol.* 26:2608-2622.

865 Degnan J.H., Rosenberg N.A. 2006. Discordance of species trees with their most likely gene  
866 trees. *PLOS Genet.* 2:e68.

867 Doyle J.J., Doyle J.L. 1987. A rapid DNA isolation procedure for small quantities of fresh  
868 leaf tissue. *Phytochem. Bull.* 19:11-15.

869 Durand E.Y., Patterson N., Reich D., Slatkin M. 2011. Testing for ancient admixture between  
870 closely related populations. *Mol. Biol. Evol.* 28:2239-2252.

871 Eaton D.A.R. 2014. PyRAD: assembly of de novo RADseq loci for phylogenetic analyses.  
872 *Bioinformatics* 30:1844-1849.

873 Eaton D.A.R., Hipp A.L., González-Rodríguez A., Cavender-Bares J. 2015. Historical  
874 introgression among the American live oaks and the comparative nature of tests for  
875 introgression. *Evolution* 69:2587-2601.

876 Eaton D.A.R., Spriggs E.L., Park B., Donoghue M.J. 2016. Misconceptions on missing data  
877 in RAD-seq phylogenetics with a deep-scale example from flowering plants. *Syst.*  
878 *Biol.* 66:399-412.

879 Ebel E.R., DaCosta J.M., Sorenson M.D., Hill R.I., Briscoe A.D., Willmott K.R., Mullen S.P.  
880 2015. Rapid diversification associated with ecological specialization in Neotropical  
881 *Adelpha* butterflies. *Mol. Ecol.* 24:2392-2405.

882 Elshire R.J., Glaubitz J.C., Sun Q., Poland J.A., Kawamoto K., Buckler E.S., Mitchell S.E.  
883 2011. A robust, simple genotyping-by-sequencing (GBS) approach for high diversity  
884 species. *PLOS ONE* 6:e19379.

885 Escudero M., Eaton D.A.R., Hahn M., Hipp A.L. 2014. Genotyping-by-sequencing as a tool  
886 to infer phylogeny and ancestral hybridization: A case study in *Carex* (Cyperaceae).  
887 *Mol. Phylogenet. Evol.* 79:359-367.

888 Farrington H.L., Lawson L.P., Clark C.M., Petren K. 2014. The evolutionary history of  
889 Darwin's finches: speciation, gene flow, and introgression in a fragmented landscape.  
890 *Evolution* 68:2932-2944.

891 Fenster C.B., Armbruster W.S., Wilson P., Dudash M.R., Thomson J.D. 2004. Pollination  
892 syndromes and floral specialization. *Annu. Rev. Ecol. Evol. Systemat.* 35:375-403.

893 Fernández-Mazuecos M., Blanco-Pastor J.L., Gómez J.M., Vargas P. 2013a. Corolla  
894 morphology influences diversification rates in bifid toadflaxes (*Linaria* sect.  
895 *Versicolores*). Ann. Bot. 112:1705-1722.

896 Fernández-Mazuecos M., Blanco-Pastor J.L., Vargas P. 2013b. A phylogeny of toadflaxes  
897 (*Linaria* Mill.) based on nuclear internal transcribed spacer sequences: systematic and  
898 evolutionary consequences. Int. J. Plant Sci. 174:234-249.

899 Fernández-Mazuecos M., Glover B.J. 2017. The evo-devo of plant speciation. Nat. Ecol.  
900 Evol. 1:0110.

901 Fernández-Mazuecos M., Vargas P. 2011. Historical isolation *versus* recent long-distance  
902 connections between Europe and Africa in bifid toadflaxes (*Linaria* sect.  
903 *Versicolores*). PLOS ONE 6:e22234.

904 Fernández-Mazuecos M., Vargas P. 2015. Quaternary radiation of bifid toadflaxes (*Linaria*  
905 sect. *Versicolores*) in the Iberian Peninsula: low taxonomic signal but high geographic  
906 structure of plastid DNA lineages. Plant Syst. Evol. 301:1411-1423.

907 Gadagkar S.R., Rosenberg M.S., Kumar S. 2005. Inferring species phylogenies from multiple  
908 genes: concatenated sequence tree versus consensus gene tree. J. Exp. Zool. B Mol.  
909 Dev. Evol. 304:64-74.

910 Giarla T.C., Esselstyn J.A. 2015. The challenges of resolving a rapid, recent radiation:  
911 empirical and simulated phylogenomics of Philippine shrews. Syst. Biol. 64:727-740.

912 Givnish T.J., Millam K.C., Mast A.R., Paterson T.B., Theim T.J., Hipp A.L., Henss J.M.,  
913 Smith J.F., Wood K.R., Sytsma K.J. 2009. Origin, adaptive radiation and  
914 diversification of the Hawaiian lobeliads (Asterales: Campanulaceae). Proc. Roy. Soc.  
915 Lond. B Biol. Sci. 276:407-416.

916 Gower J.C. 1971. A general coefficient of similarity and some of its properties. Biometrics  
917 27:857-874.

918 Grabowski P.P., Morris G.P., Casler M.D., Borevitz J.O. 2014. Population genomic variation  
919 reveals roles of history, adaptation and ploidy in switchgrass. *Mol. Ecol.* 23:4059-  
920 4073.

921 Guzmán B., Lledó M.D., Vargas P. 2009. Adaptive radiation in Mediterranean *Cistus*  
922 (*Cistaceae*). *PLOS ONE* 4:e6362.

923 Hamon P., Grover C.E., Davis A.P., Rakotomalala J.J., Raharimalala N.E., Albert V.A.,  
924 Sreenath H.L., Stoffelen P., Mitchell S.E., Couturon E., Hamon S., de Kochko A.,  
925 Crouzillat D., Rigoreau M., Sumirat U., Akaffou S., Guyot R. 2017. Genotyping-by-  
926 sequencing provides the first well-resolved phylogeny for coffee (*Coffea*) and insights  
927 into the evolution of caffeine content in its species: GBS coffee phylogeny and the  
928 evolution of caffeine content. *Mol. Phylogenet. Evol.* 109:351-361.

929 Harvey M.G., Judy C.D., Seeholzer G.F., Maley J.M., Graves G.R., Brumfield R.T. 2015.  
930 Similarity thresholds used in DNA sequence assembly from short reads can reduce the  
931 comparability of population histories across species. *PeerJ* 3:e895.

932 Harvey M.G., Smith B.T., Glenn T.C., Faircloth B.C., Brumfield R.T. 2016. Sequence  
933 capture versus restriction site associated DNA sequencing for shallow systematics.  
934 *Syst. Biol.* 65:910-924.

935 Heled J., Drummond A.J. 2010. Bayesian inference of species trees from multilocus data.  
936 *Mol. Biol. Evol.* 27:570-580.

937 Hipp A.L. 2014. RADami: R package for phylogenetic analysis of RADseq data. Available in  
938 <https://cran.r-project.org/web/packages/RADami/index.html>.

939 Hipp A.L., Eaton D.A.R., Cavender-Bares J., Fitzek E., Nipper R., Manos P.S. 2014. A  
940 framework phylogeny of the American oak clade based on sequenced RAD data.  
941 *PLOS ONE* 9:e93975.

942 Huang H., Knowles L.L. 2014. Unforeseen consequences of excluding missing data from  
943 next-generation sequences: simulation study of RAD sequences. *Syst. Biol.* 65:357-  
944 365.

945 Hughes C., Eastwood R. 2006. Island radiation on a continental scale: exceptional rates of  
946 plant diversification after uplift of the Andes. *P. Natl. Acad. Sci. USA* 103:10334-  
947 10339.

948 Kampstra P. 2008. Beanplot: A boxplot alternative for visual comparison of distributions. *J.*  
949 *Stat. Softw.* 28:1-9.

950 Kay K.M., Voelckel C., Yang J.Y., Hufford K.M., Kaska D.D., Hodges S.A. 2006. Floral  
951 characters and species diversification. In: Harder L.D., Barrett S.C.H., editors.  
952 *Ecology and evolution of flowers*, Oxford: Oxford University Press. pp. 311-325.

953 Kubatko L.S., Degnan J.H. 2007. Inconsistency of phylogenetic estimates from concatenated  
954 data under coalescence. *Syst. Biol.* 56:17-24.

955 Kumar S., Filipski A.J., Battistuzzi F.U., Pond S.L.K., Tamura K. 2011. Statistics and truth in  
956 phylogenomics. *Mol. Biol. Evol.* 29:457-472.

957 Leaché A.D., Banbury B.L., Felsenstein J., de Oca A.N.-M., Stamatakis A. 2015a. Short tree,  
958 long tree, right tree, wrong tree: new acquisition bias corrections for inferring SNP  
959 phylogenies. *Syst. Biol.* 64:1032-1047.

960 Leaché A.D., Chavez A.S., Jones L.N., Grummer J.A., Gottscho A.D., Linkem C.W. 2015b.  
961 Phylogenomics of phrynosomatid lizards: conflicting signals from sequence capture  
962 versus restriction site associated DNA sequencing. *Genome Biol. Evol.* 7:706-719.

963 Lemmon E.M., Lemmon A.R. 2013. High-throughput genomic data in systematics and  
964 phylogenetics. *Annu. Rev. Ecol. Evol. Systemat.* 44:99-121.

965 Li H., Ruan J., Durbin R. 2008. Mapping short DNA sequencing reads and calling variants  
966 using mapping quality scores. *Genome Res.* 18:1851-1858.

967 Liu L. 2008. BEST: Bayesian estimation of species trees under the coalescent model.  
968 Bioinformatics 24:2542-2543.

969 Liu L., Wu S., Yu L. 2015. Coalescent methods for estimating species trees from  
970 phylogenomic data. J. Syst. Evol. 53:380-390.

971 Liu L., Yu L. 2010. Phybase: an R package for species tree analysis. Bioinformatics 26:962-  
972 963.

973 Liu L., Yu L. 2011. Estimating species trees from unrooted gene trees. Syst. Biol. 60:661-  
974 667.

975 Maddison W.P., Maddison D.R. 2011. Mesquite: a modular system for evolutionary analysis.  
976 Available in <http://mesquiteproject.org>.

977 Mahler D.L., Ingram T., Revell L.J., Losos J.B. 2013. Exceptional convergence on the  
978 macroevolutionary landscape in island lizard radiations. Science 341:292-295.

979 Mallo D. 2015. Multi-locus bootstrapping script. Available in  
980 <https://github.com/adamallo/multi-locus-bootstrapping>.

981 Mallo D. 2016. NJstM. Available in <https://github.com/adamallo/NJstM>.

982 Manthey J.D., Campillo L.C., Burns K.J., Moyle R.G. 2016. Comparison of target-capture  
983 and restriction-site associated DNA sequencing for phylogenomics: a test in  
984 cardinalid tanagers (Aves, Genus: *Piranga*). Syst. Biol. 65:640-650.

985 Mastretta-Yanes A., Arrigo N., Alvarez N., Jorgensen T.H., Piñero D., Emerson B.C. 2015.  
986 Restriction site-associated DNA sequencing, genotyping error estimation and de novo  
987 assembly optimization for population genetic inference. Mol. Ecol. Resour. 15:28-41.

988 McCormack J.E., Hird S.M., Zellmer A.J., Carstens B.C., Brumfield R.T. 2013. Applications  
989 of next-generation sequencing to phylogeography and phylogenetics. Mol.  
990 Phylogenet. Evol. 66:526-538.

991 Meiklejohn K.A., Faircloth B.C., Glenn T.C., Kimball R.T., Braun E.L. 2016. Analysis of a  
992 rapid evolutionary radiation using ultraconserved elements: evidence for a bias in  
993 some multispecies coalescent methods. *Syst. Biol.* 65:612-627.

994 Mirarab S., Bayzid M.S., Warnow T. 2016. Evaluating summary methods for multilocus  
995 species tree estimation in the presence of incomplete lineage sorting. *Syst. Biol.*  
996 65:366-380.

997 Mirarab S., Reaz R., Bayzid M.S., Zimmermann T., Swenson M.S., Warnow T. 2014.  
998 ASTRAL: genome-scale coalescent-based species tree estimation. *Bioinformatics*  
999 30:i541-i548.

1000 Mittelbach G.G., Schemske D.W. 2015. Ecological and evolutionary perspectives on  
1001 community assembly. *Trends Ecol. Evol.* 30:241-247.

1002 Muschick M., Indermaur A., Salzburger W. 2012. Convergent evolution within an adaptive  
1003 radiation of cichlid fishes. *Curr. Biol.* 22:2362-2368.

1004 Nadeau N.J., Martin S.H., Kozak K.M., Salazar C., Dasmahapatra K.K., Davey J.W., Baxter  
1005 S.W., Blaxter M.L., Mallet J., Jiggins C.D. 2013. Genome-wide patterns of  
1006 divergence and gene flow across a butterfly radiation. *Mol. Ecol.* 22:814-826.

1007 Nicotra A.B., Chong C., Bragg J.G., Ong C.R., Aitken N.C., Chuah A., Lepschi B., Borevitz  
1008 J.O. 2016. Population and phylogenomic decomposition via genotyping-by-  
1009 sequencing in Australian *Pelargonium*. *Mol. Ecol.* 25:2000-2014.

1010 Nieto Feliner G., Álvarez I., Fuertes-Aguilar J., Heuertz M., Marques I., Moharrek F., Piñeiro  
1011 R., Riina R., Rosselló J.A., Soltis P.S., Villa-Machío I. 2017. Is homoploid hybrid  
1012 speciation that rare? An empiricist's view. *Heredity* 118:513-516.

1013 Oksanen J., Blanchet F.G., Kindt R., Legendre P., O'Hara R.B., Simpson G.L., Solymos P.,  
1014 M.H.H. S., Wagner H. 2011. *vegan*: Community Ecology Package. R package version  
1015 1.17-9. Available in <http://CRAN.R-project.org/package=vegan>.

1016 Paradis E., Claude J., Strimmer K. 2004. APE: analyses of phylogenetics and evolution in R  
1017 language. *Bioinformatics* 20:289-290.

1018 Peterson B.K., Weber J.N., Kay E.H., Fisher H.S., Hoekstra H.E. 2012. Double digest  
1019 RADseq: an inexpensive method for de novo SNP discovery and genotyping in model  
1020 and non-model species. *PLOS ONE* 7:e37135.

1021 Poland J.A., Brown P.J., Sorrells M.E., Jannink J.L. 2012. Development of high-density  
1022 genetic maps for barley and wheat using a novel two-enzyme genotyping-by-  
1023 sequencing approach. *PLOS ONE* 7:e32253.

1024 Pritchard J.K., Stephens M., Donnelly P. 2000. Inference of population structure using  
1025 multilocus genotype data. *Genetics* 155:945-959.

1026 R Development Core Team. 2016. R: A language and environment for statistical computing.  
1027 Vienna: R Foundation for Statistical Computing.

1028 Ree R.H., Hipp A.L. 2015. Inferring phylogenetic history from restriction site associated  
1029 DNA (RADseq). In: Hörandl E., Appelhans M.S., editors. *Next-generation*  
1030 *sequencing in plant systematics*, Königstein: Koeltz Scientific Books. pp. 181-204.

1031 Revell L.J. 2012. phytools: an R package for phylogenetic comparative biology (and other  
1032 things). *Methods Ecol. Evol.* 3:217-223.

1033 Roure B., Baurain D., Philippe H. 2013. Impact of missing data on phylogenies inferred from  
1034 empirical phylogenomic data sets. *Mol. Biol. Evol.* 30:197-214.

1035 Rubin B.E.R., Ree R.H., Moreau C.S. 2012. Inferring phylogenies from RAD sequence data.  
1036 *PLOS ONE* 7:e33394.

1037 Sáez L., Bernal M. 2009. *Linaria* Mill. In: Castroviejo S., Herrero A., Benedí C., Rico E.,  
1038 Güemes J., editors. *Flora iberica XIII (Plantaginaceae – Scrophulariaceae)*, Madrid:  
1039 CSIC. pp. 232-324.

- 1040 Salichos L., Rokas A. 2013. Inferring ancient divergences requires genes with strong  
1041 phylogenetic signals. *Nature* 497:327-331.
- 1042 Sang T. 2002. Utility of low-copy nuclear gene sequences in plant phylogenetics. *Crit. Rev.*  
1043 *Biochem. Mol.* 37:121-147.
- 1044 Schluter D. 2000. *The ecology of adaptive radiation*. Oxford: Oxford University Press.
- 1045 Seehausen O. 2006. African cichlid fish: a model system in adaptive radiation research. *Proc.*  
1046 *Roy. Soc. Lond. B Biol. Sci.* 273:1987-1998.
- 1047 Seo T.K. 2008. Calculating bootstrap probabilities of phylogeny using multilocus sequence  
1048 data. *Mol. Biol. Evol.* 25:960-971.
- 1049 Shafer A., Peart C.R., Tusso S., Maayan I., Brelsford A., Wheat C.W., Wolf J.B.W. 2016.  
1050 Bioinformatic processing of RAD-seq data dramatically impacts downstream  
1051 population genetic inference. *Methods Ecol. Evol.* doi 10.1111/2041-210X.12700.
- 1052 Shaffer H.B., Thomson R.C. 2007. Delimiting species in recent radiations. *Syst. Biol.*  
1053 56:896-906.
- 1054 Shaw J., Lickey E.B., Schilling E.E., Small R.L. 2007. Comparison of whole chloroplast  
1055 genome sequences to choose noncoding regions for phylogenetic studies in  
1056 angiosperms: the tortoise and the hare III. *Am. J. Bot.* 94:275-288.
- 1057 Shaw K.L. 2002. Conflict between nuclear and mitochondrial DNA phylogenies of a recent  
1058 species radiation: what mtDNA reveals and conceals about modes of speciation in  
1059 Hawaiian crickets. *P. Natl. Acad. Sci. USA* 99:16122-16127.
- 1060 Shimodaira H. 2002. An approximately unbiased test of phylogenetic tree selection. *Syst.*  
1061 *Biol.* 51:492-508.
- 1062 Shimodaira H., Hasegawa M. 1999. Multiple comparisons of log-likelihoods with  
1063 applications to phylogenetic inference. *Mol. Biol. Evol.* 16:1114-1116.

- 1064 Shimodaira H., Hasegawa M. 2001. CONSEL: for assessing the confidence of phylogenetic  
1065 tree selection. *Bioinformatics* 17:1246-1247.
- 1066 Sidlauskas B. 2008. Continuous and arrested morphological diversification in sister clades of  
1067 characiform fishes: a phylomorphospace approach. *Evolution* 62:3135-3156.
- 1068 Solís-Lemus C., Ané C. 2016. Inferring phylogenetic networks with maximum  
1069 pseudolikelihood under incomplete lineage sorting. *PLOS Genet.* 12:e1005896.
- 1070 Solís-Lemus C., Yang M., Ané C. 2016. Inconsistency of species-tree methods under gene  
1071 flow. *Syst. Biol.* 65:843-851.
- 1072 Stamatakis A. 2006. Phylogenetic models of rate heterogeneity: a high performance  
1073 computing perspective. *Proceedings of the IPDPS2006, Rhodos, Greece: IEEE.*
- 1074 Stamatakis A. 2014. RAxML version 8: a tool for phylogenetic analysis and post-analysis of  
1075 large phylogenies. *Bioinformatics* 30:1312-1313.
- 1076 Suchan T., Pitteloud C., Gerasimova N.S., Kostikova A., Schmid S., Arrigo N., Pajkovic M.,  
1077 Ronikier M., Alvarez N. 2016. Hybridization capture using RAD probes (hyRAD), a  
1078 new tool for performing genomic analyses on collection specimens. *PLOS ONE*  
1079 11:e0151651.
- 1080 Sutton D.A. 1988. A revision of the tribe Antirrhineae. Oxford: Oxford University Press.
- 1081 Swofford D. 2002. PAUP\*. Phylogenetic analysis using parsimony (\*and other methods).  
1082 Version 4. Sunderland, Massachusetts: Sinauer.
- 1083 Takahashi T., Nagata N., Sota T. 2014. Application of RAD-based phylogenetics to complex  
1084 relationships among variously related taxa in a species flock. *Mol. Phylogenet. Evol.*  
1085 80:137-144.
- 1086 Valdés B. 1970. Taxonomía experimental del género *Linaria* IV. Reproducción sexual:  
1087 autogamia y polinización intraespecífica. *Bol. R. Soc. Esp. Hist. Nat. Secc. Biol.*  
1088 68:79-89.

1089 Valente L.M., Savolainen V., Vargas P. 2010. Unparalleled rates of species diversification in  
1090 Europe. Proc. Roy. Soc. Lond. B Biol. Sci. 277:1489-1496.

1091 van Orsouw N.J., Hogers R.C.J., Janssen A., Yalcin F., Snoeijers S., Verstege E., Schneiders  
1092 H., van der Poel H., Van Oeveren J., Verstegen H. 2007. Complexity reduction of  
1093 polymorphic sequences (CRoPS™): a novel approach for large-scale polymorphism  
1094 discovery in complex genomes. PLOS ONE 2:e1172.

1095 Vargas P., Zardoya R. 2014. The tree of life: evolution and classification of living organisms.  
1096 Sunderland, Massachusetts: Sinauer Associates Inc.

1097 Venables W.N., Ripley B.D. 2002. Modern applied statistics with S. 4th edition. New York:  
1098 Springer.

1099 Vigalondo B., Fernández-Mazuecos M., Vargas P., Sáez L. 2015. Unmasking cryptic species:  
1100 morphometric and phylogenetic analyses of the Ibero-North African *Linaria*  
1101 *incarnata* complex. Bot. J. Linn. Soc. 177:395-417.

1102 Wagner C.E., Keller I., Wittwer S., Selz O.M., Mwaiko S., Greuter L., Sivasundar A.,  
1103 Seehausen O. 2013. Genome-wide RAD sequence data provide unprecedented  
1104 resolution of species boundaries and relationships in the Lake Victoria cichlid  
1105 adaptive radiation. Mol. Ecol. 22:787-798.

1106 Waterhouse A.M., Procter J.B., Martin D.M.A., Clamp M., Barton G.J. 2009. Jalview  
1107 Version 2—a multiple sequence alignment editor and analysis workbench.  
1108 Bioinformatics 25:1189-1191.

1109 Whittall J.B., Voelckel C., Kliebenstein D.J., Hodges S.A. 2006. Convergence, constraint and  
1110 the role of gene expression during adaptive radiation: floral anthocyanins in  
1111 *Aquilegia*. Mol. Ecol. 15:4645-4657.

1112

1113

1114

1115           FIGURE CAPTIONS

1116           FIGURE 1. Results of morphometric and genetic structure analyses of the eight taxa  
1117 included in the Iberian clade of *Linaria* subsect. *Versicolores* (see Table 1 for the meaning of  
1118 acronyms). (a) Morphospace based on principal coordinate analysis of all morphometric data  
1119 (24 quantitative and 3 qualitative variables; 166 individuals); values of the first three  
1120 coordinates, explaining 54.8% of variance, are represented. (b) Morphospace based on  
1121 discriminant function analysis of quantitative variables; values of the first three canonical  
1122 discriminant functions, explaining 79.5% of variation among groups, are represented. (c)  
1123 Principal component analysis based on the unlinked single nucleotide polymorphism (SNP)  
1124 matrix obtained from the c85m4 dataset (5265 SNPs; 76 individuals); values of coordinates 1,  
1125 2 and 4, explaining 72.1% of variance, are represented. In all panels, 95% confidence ellipses  
1126 of concentration for each of the eight species are shown, and arrows indicate CRA  
1127 individuals (ultimately assigned to SPA; see text).

1128

1129

1130           FIGURE 2. Results from concatenation- and coalescent-based phylogenetic analyses of  
1131 genotyping-by-sequencing datasets of the Iberian clade of *Linaria* subsect. *Versicolores*. (a-d)  
1132 Four alternative maximum-likelihood (ML) phylogenetic trees obtained in RAxML from  
1133 concatenated analyses of datasets assembled using different clustering thresholds: c84m4 (a),  
1134 c85m4 (b), c87m4 (c), c92m4 (d) (see Table 2). Numbers above branches are percentage  
1135 bootstrap values from ML analyses. Numbers below branches are posterior probabilities from  
1136 Bayesian analyses in ExaBayes. (e) Coalescent-based species tree obtained using the NJ<sub>st</sub>  
1137 method, after estimation of unrooted gene trees by ML in RAxML with 100 bootstrap  
1138 replicates. The 50% majority-rule consensus of 50 multilocus bootstrap replicates is shown.  
1139 The same majority-rule topology was obtained from four genotyping-by-sequencing datasets

1140 assembled using different clustering thresholds (c84m4, c85m4, c87m4, c92m4; see Table 2).  
1141 Numbers above branches are multilocus bootstrap support values (in percentage) from the  
1142 c84m4 and c85m4 datasets. Numbers below branches are multilocus bootstrap support values  
1143 from the c87m4 and c92m4 datasets. (f) Coalescent-based species tree obtained using the  
1144 SVDquartets method with 100 bootstrap replicates. The 50% majority-rule consensus  
1145 obtained from the same four datasets is shown. Numbers above branches are bootstrap  
1146 support values from the c84m4 and c85m4 datasets. Numbers below branches are bootstrap  
1147 support values from the c87m4 and c92m4 datasets. (g-h) Fixed network topologies evaluated  
1148 in a coalescent with hybridisation framework using the SNaQ method: a network with the  
1149  $NJ_{st}$  tree as major vertical inheritance pattern (MVIP) and reticulations representing  
1150 incongruences with the SVDquartets tree (g), and a network with the SVDquartets tree as  
1151 MVIP and reticulations representing incongruences with the  $NJ_{st}$  tree (h). The four values  
1152 attached to hybrid edges represent inheritance probabilities (i.e. the proportions of genes  
1153 contributed by each parental population to a hybrid taxon) estimated from the c84m4, c85m4,  
1154 c87m4 and c92m4 datasets respectively.

1155

1156         FIGURE 3. Numbers of loci supporting and disfavouring constrained concatenated  
1157 trees with eight alternative topologies (1-8, left) in four genotyping-by-sequencing datasets  
1158 assembled using different clustering thresholds (c84m4, c85m4, c87m4, c92m4; right; see  
1159 Table 2). Topologies 1-4 are the four alternative optimal topologies respectively produced by  
1160 concatenated analyses of the same four datasets (see Fig. 3a-d). Topology 5 is the one  
1161 produced by coalescent-based analyses of all four datasets in  $NJ_{st}$  (see Fig. 3e). Topology 6 is  
1162 the one produced by coalescent-based analyses of all four datasets in SVDquartets (see Fig.  
1163 3f). Topologies 7 and 8 were produced by previously published concatenated (topology 7)  
1164 and coalescent-based (topology 8) analyses of combined ITS and ptDNA sequences

1165 (Fernández-Mazuecos et al. 2013a; Vigalondo et al. 2015). For each dataset, numbers of loci  
1166 significantly supporting and disfavouring each tree topology are plotted against the log-  
1167 likelihood of the tree when using the full concatenated matrix. Black dots represent the  
1168 maximum likelihood tree for each dataset. White dots represent constrained trees that were  
1169 significantly rejected by Shimodaira–Hasegawa tests, and grey dots represent constrained  
1170 trees that were not significantly rejected (see Table 3).

1171

1172           FIGURE 4. Patterns of morphological evolution in the Iberian clade of *Linaria* subsect.  
1173 *Versicolores* based on coalescent-based phylogenetic analysis of genotyping-by-sequencing  
1174 data. (a) Coalescent-based species tree obtained using the NJ<sub>st</sub> method, with dotted lines  
1175 representing the alternative position of two species in the SVDquartets tree. Flowers of the  
1176 eight species of the Iberian clade of *Linaria* subsect. *Versicolores* are shown (photos by J.  
1177 Ramírez and M. Fernández-Mazuecos), and mean values of spur length and tube width  
1178 according to Fernández-Mazuecos et al. (2013a) are plotted. (b) Phylomorphospace defined  
1179 by the NJ<sub>st</sub> phylogeny and the first three canonical discriminant functions of the  
1180 morphometric analysis based on vegetative and reproductive traits. Each species is  
1181 represented by the mean values of the coordinates. (c) Phylomorphospace defined by the NJ<sub>st</sub>  
1182 phylogeny and the first two canonical variates of a previously published geometric  
1183 morphometric analysis of flowers (Fernández-Mazuecos et al. 2013a).

1184

1185           FIGURE 5. Biogeographic patterns in the Iberian clade of *Linaria* subsect. *Versicolores*  
1186 based on coalescent-based phylogenetic analysis of genotyping-by-sequencing data. The NJ<sub>st</sub>  
1187 species tree is projected onto the geographic distribution of the eight species in the Iberian  
1188 Peninsula. Dashed lines at the limit between *L. spartea* and *L. viscosa* indicate uncertainty on  
1189 distribution ranges.

1190

1191

## TABLES

1192

TABLE 1. Study taxa and summary of plant materials included in morphometric and

1193

genotyping-by-sequencing (GBS) analyses.

Taxon <sup>a</sup>	Acronym	No. sampled individuals, morphometry	No. sampled individuals, GBS <sup>b</sup>	No. loci (mean $\pm$ SD) <sup>c</sup>
<i>Linaria</i> subsect. <i>Elegantes</i> (2/2)	OUT	-	4 / 4	2130 $\pm$ 296
<i>Linaria</i> subsect. <i>Versicolores</i> , North African clade (6/20)	NAF	-	9 / 9	2524 $\pm$ 618
<i>Linaria</i> subsect. <i>Versicolores</i> , Iberian clade (8/8)	-	-	76 / 68	3586 $\pm$ 1048
<i>L. algarviana</i> Chav.	ALG	17	10 / 10	3219 $\pm$ 808
<i>L. becerrae</i> Blanca, Cueto & J.Fuentes	BEC	11	8 / 8	4464 $\pm$ 706
<i>L. clementei</i> Haens.	CLE	10	9 / 9	4229 $\pm$ 845
<i>L. incarnata</i> (Vent.) Spreng.	INC	33	10 / 10	3526 $\pm$ 670
<i>L. onubensis</i> Pau	ONU	32	9 / 8	3805 $\pm$ 668
<i>L. salzmännii</i> Boiss. (= <i>L. viscosa</i> subsp. <i>spicata</i> (Kunze) D.A.Sutton)	SAL	21	10 / 10	3801 $\pm$ 875
<i>L. spartea</i> (L.) Chaz.	SPA	27	10 / 8	3213 $\pm$ 1218
<i>L. viscosa</i> (L.) Chaz.	VIS	22	10 / 5	2630 $\pm$ 1412

1194

Notes: The final taxonomic treatment is followed, with a previous treatment in brackets for *L. salzmännii*. The

1195

specimens sampled in the *locus classicus* of *L. viscosa* subsp. *crassifolia* (CRA) are included in *L. spartea* (see

1196

text).

1197

<sup>a</sup>Sampled/total numbers of species and subspecies for the three major clades are shown in brackets.

1198

<sup>b</sup>For each taxon, total number of sampled individuals / number of individuals included in phylogenetic analyses

1199

is shown.

1200

<sup>c</sup>For each taxon, the mean ( $\pm$ SD) number of loci recovered across individuals and pyRAD assemblies (from

1201

clustering threshold 0.80 to 0.95, with minimum taxon coverage of 4) is shown. Figures calculated after

1202

taxonomic reassignment of some individuals resulting from genetic structure analyses.

1203

1204

1205

1206

1207 TABLE 2. Characteristics of assembled genotyping-by-sequencing datasets generated  
 1208 in pyRAD and used in phylogenetic analyses (81 individuals).

<b>Dataset</b>	<b>Clustering threshold</b>	<b>Minimum taxon coverage</b>	<b>No. loci</b>	<b>Concatenated length (bp)</b>	<b>% Missing data</b>	<b>No. PICs</b>
c84m4	0.84	4	22106	2039028	85.50	81001
c84m10	0.84	10	9090	850257	74.72	57815
c84m20	0.84	20	3888	367013	62.18	32559
c85m4	0.85	4	22586	2079729	85.62	80502
c85m10	0.85	10	9203	858302	74.81	57033
c85m20	0.85	20	3894	366417	62.24	31842
c87m4	0.87	4	23593	2166830	85.91	78488
c87m10	0.87	10	9475	880128	75.28	54553
c87m20	0.87	20	3881	363324	62.65	29259
c92m4	0.92	4	29037	2647482	86.90	72514
c92m10	0.92	10	10738	986997	76.42	47175
c92m20	0.92	20	3899	359814	63.09	22620

1209 *Notes:* Assembly parameters, dataset sizes, completeness and numbers of parsimony-informative characters  
 1210 (PICs) are indicated.

1211

TABLE 3. Results from topology tests in CONSEL.

Dataset	Rank	Topology	Obs.	AU	SH	WSH
c84m4	1	1	-32.5	0.841	0.98	0.985
	2	4	32.5	0.466	0.825	0.758
	3	2	59.2	0.262	0.752	0.511
	4	3	76.7	0.244	0.663	0.57
	5	5	164.2	0.102	0.398	0.251
	6	6	239.1	0.061	0.207	0.195
	7	8	978.7	1.00E-07*	0*	0*
	8	7	6270.7	2.00E-08*	0*	0*
c85m4	1	2	-29.9	0.823	0.986	0.991
	2	5	29.9	0.365	0.791	0.694
	3	3	46.1	0.335	0.746	0.647
	4	1	85.1	0.12	0.615	0.294
	5	4	137	0.063	0.411	0.247
	6	6	456.7	0.001*	0.004*	0.001*
	7	8	1055	1.00E-04*	0*	0*
	8	7	6398.8	4.00E-05*	0*	0*
c87m4	1	3	-61.4	0.897	0.991	0.997
	2	4	61.4	0.205	0.69	0.489
	3	2	71.4	0.228	0.655	0.477
	4	1	115.5	0.137	0.491	0.356
	5	5	182.4	0.015*	0.287	0.099
	6	6	442.4	1.00E-04*	0.005*	2.00E-04*
	7	8	1323.9	1.00E-06*	0*	0*
	8	7	6279	2.00E-06*	0*	0*
c92m4	1	4	-75.7	0.89	0.993	0.996
	2	1	75.7	0.198	0.64	0.496
	3	3	77	0.173	0.639	0.435
	4	2	155.7	0.033*	0.346	0.174
	5	5	268.1	0.005*	0.136	0.027*
	6	6	488.9	4.00E-11*	0.004*	0*
	7	8	1282.5	3.00E-24*	0*	0*
	8	7	5344.1	5.00E-08*	0*	0*

Notes: Four genotyping-by-sequencing datasets were used to test eight alternative topologies in a maximum likelihood framework with concatenated matrices. Tested topologies (summarized in Fig. 3) included the four alternative optimal topologies produced by concatenated analyses of the same four datasets (topologies 1-4; Fig. 2a-d), the topologies produced by coalescent-based  $NJ_{st}$  (topology 5; Fig. 2e) and SVDquartets (topology 6; Fig. 2f) analyses of all four datasets and two topologies produced by previously-published analyses of internal transcribed spacer and plastid DNA sequences (topologies 7, 8). For each dataset, topologies are ranked by the test statistics (Obs.), and  $p$ -values of the Approximately Unbiased (AU), Shimodaira–Hasegawa (SH) and Weighted Shimodaira–Hasegawa (WSH) tests are shown. Asterisks indicate significant results ( $p < 0.05$ ).

TABLE 4. *D*-statistic tests conducted on four genotyping-by-sequencing datasets given a four-taxon tree (((P1,P2),P3),O).

Dataset	Set	Assumed species tree	P1	P2	P3	O	N	% Sig. (ABBA>BABA)	% Sig. (BABA>ABBA)
c84m4	1	NJ <sub>st</sub>	ALG, INC	SPA	VIS, ONU	BEC, SAL	648	9.26	3.55
	2	NJ <sub>st</sub>	CLE	BEC	SAL	VIS, ONU, ALG, SPA, INC	405	23.95	0
	3	SVDquartets	VIS, ONU	SPA	INC	BEC, SAL	324	25.00	0.31
	4	SVDquartets	ALG, INC, SPA, VIS, ONU	BEC	CLE	NAF	540	22.59	0.00
c85m4	1	NJ <sub>st</sub>	ALG, INC	SPA	VIS, ONU	BEC, SAL	648	8.33	2.31
	2	NJ <sub>st</sub>	CLE	BEC	SAL	VIS, ONU, ALG, SPA, INC	405	27.16	0
	3	SVDquartets	VIS, ONU	SPA	INC	BEC, SAL	324	24.07	0.62
	4	SVDquartets	ALG, INC, SPA, VIS, ONU	BEC	CLE	NAF	540	34.63	0.00
c87m4	1	NJ <sub>st</sub>	ALG, INC	SPA	VIS, ONU	BEC, SAL	648	11.11	5.40
	2	NJ <sub>st</sub>	CLE	BEC	SAL	VIS, ONU, ALG, SPA, INC	405	29.88	0
	3	SVDquartets	VIS, ONU	SPA	INC	BEC, SAL	324	38.27	0.31
	4	SVDquartets	ALG, INC, SPA, VIS, ONU	BEC	CLE	NAF	540	17.96	0.74
c92m4	1	NJ <sub>st</sub>	ALG, INC	SPA	VIS, ONU	BEC, SAL	648	12.65	2.01
	2	NJ <sub>st</sub>	CLE	BEC	SAL	VIS, ONU, ALG, SPA, INC	405	5.68	1.73
	3	SVDquartets	VIS, ONU	SPA	INC	BEC, SAL	324	41.36	0.31
	4	SVDquartets	ALG, INC, SPA, VIS, ONU	BEC	CLE	NAF	540	18.89	0.93

*Notes:* Three individuals per species of the Iberian clade and four individuals from different species of the North African clade were selected, and introgression hypotheses potentially explaining topological differences between the two species trees obtained in coalescent-based analyses (Fig. 2e, f) were tested. For each set of tests, we show the number of tests conducted using different combinations of individuals (N) and the percentage of significant tests ( $p < 0.05$ ) for ABBA>BABA (potential introgression between P2 and P3) and BABA>ABBA (potential introgression between P1 and P3).

TABLE 5. Results from tree and network evaluation using the SNaQ method.

	NJ <sub>st</sub> tree without reticulations	SVDquartets tree without reticulations	NJ <sub>st</sub> tree with reticulations	SVDquartets tree with reticulations
c84m4	734.72	1084.15	736.67	732.19
c85m4	758.05	1120.34	761.38	801.18
c87m4	817.74	1201.44	829.88	896.67
c92m4	1547.23	1648.7	1166.42	1406.25

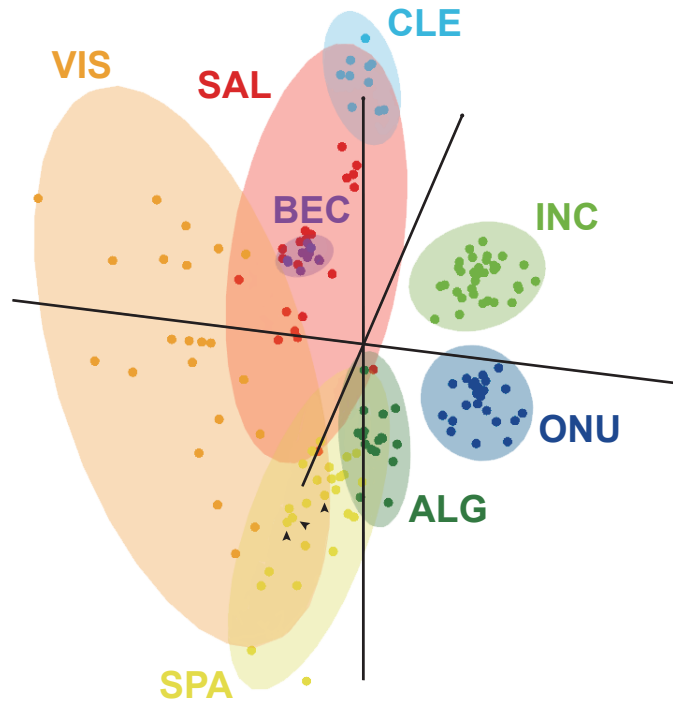
*Notes:* Four reduced datasets with 27 individuals were used to evaluate four fixed topologies, including the NJ<sub>st</sub> and SVDquartets species tree topologies without reticulations (Figs. 2e, f), the NJ<sub>st</sub> tree as major vertical inheritance pattern (MVIP) with reticulations representing incongruences with the SVDquartets tree (Fig. 2g), and the SVDquartets tree as MVIP with hybrid edges representing incongruences with the NJ<sub>st</sub> tree (Fig. 2h). Pseudo-deviance values are shown, with lower values indicating a better fit.

## SUPPLEMENTARY MATERIAL

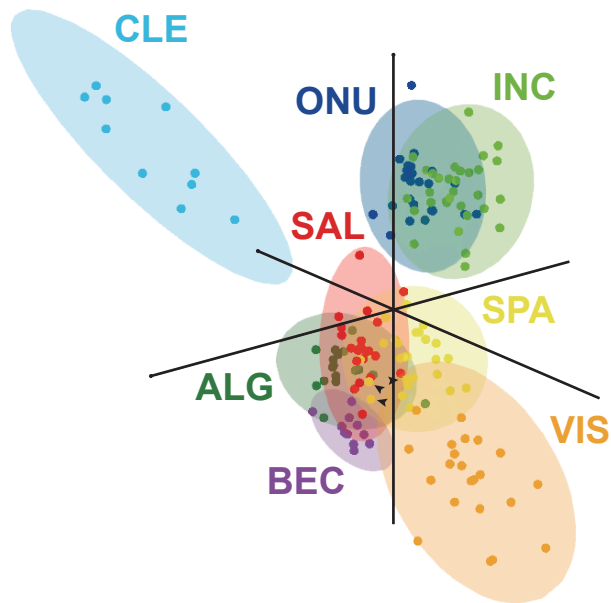
Supplementary material, including data files and online-only appendices, can be found in the Dryad data repository at

<http://datadryad.org/review?doi=doi:10.5061/dryad.mp818>

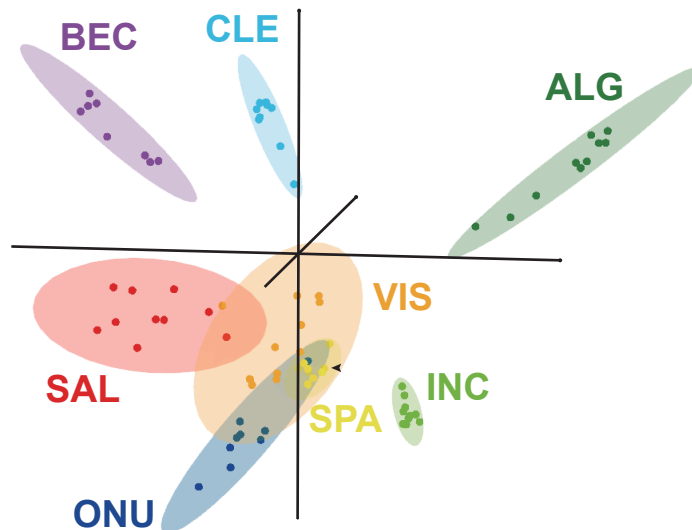
### a) Morphology (PCoA)



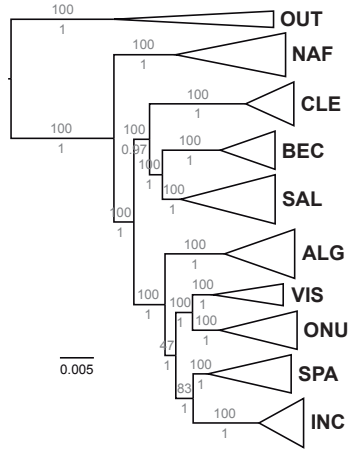
### b) Morphology (DFA)



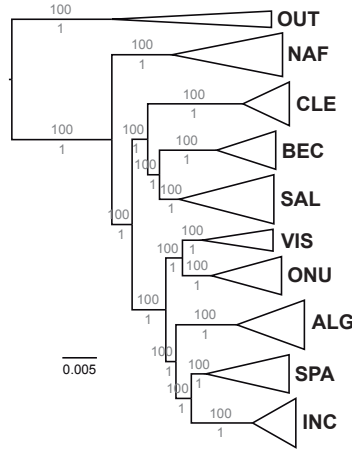
### c) SNPs (PCA)



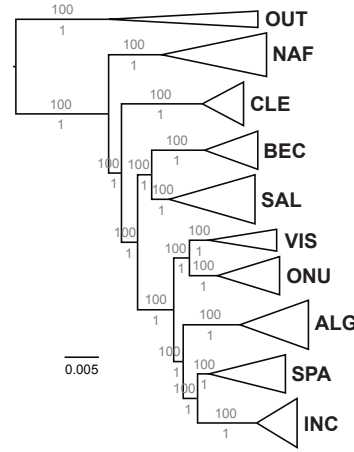
**a) Concatenated, RAxML/ExaBayes**  
**TOPOLOGY 1 (c84m4)**



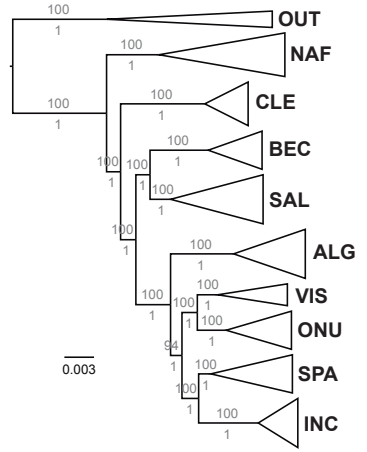
**b) Concatenated, RAxML/ExaBayes**  
**TOPOLOGY 2 (c85m4)**



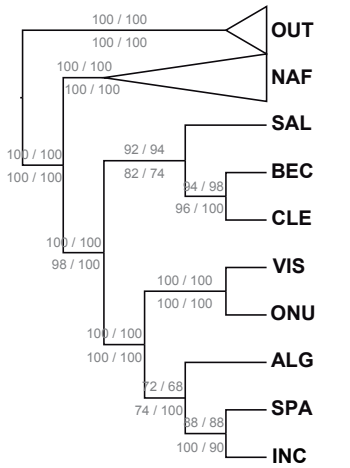
**c) Concatenated, RAxML/ExaBayes**  
**TOPOLOGY 3 (c87m4)**



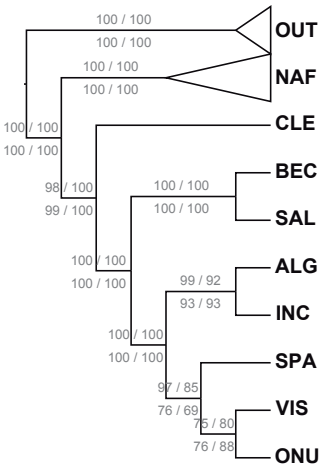
**d) Concatenated, RAxML/ExaBayes**  
**TOPOLOGY 4 (c92m4)**



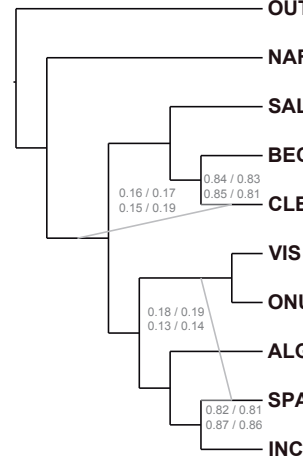
**e) Coalescent, NJst**  
**TOPOLOGY 5 (4 datasets)**



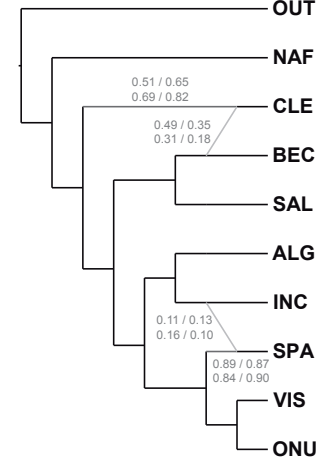
**f) Coalescent, SVDquartets**  
**TOPOLOGY 6 (4 datasets)**

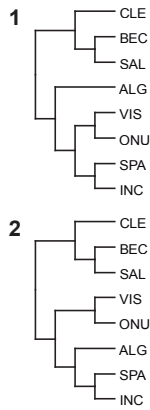


**g) Coalescent with hybridisation, SNaQ**  
**TOPOLOGY 5 fixed as MVIP (4 datasets)**

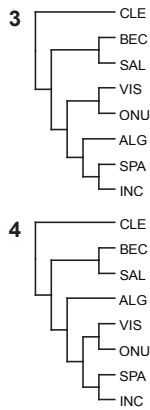
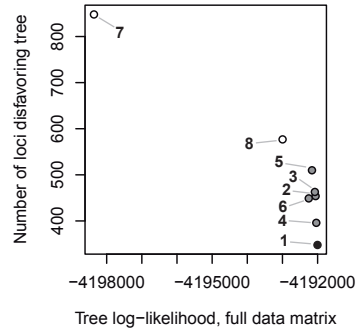
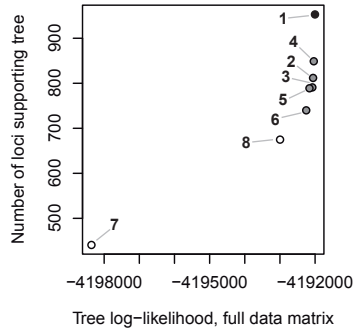


**h) Coalescent with hybridisation, SNaQ**  
**TOPOLOGY 6 fixed as MVIP (4 datasets)**

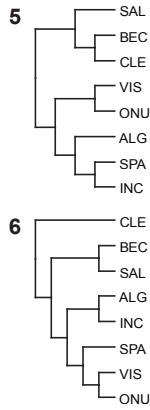
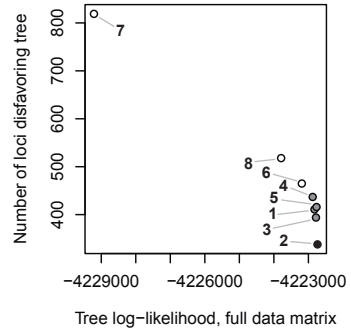
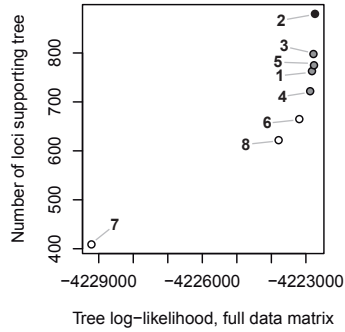




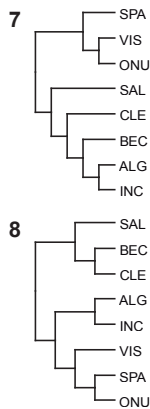
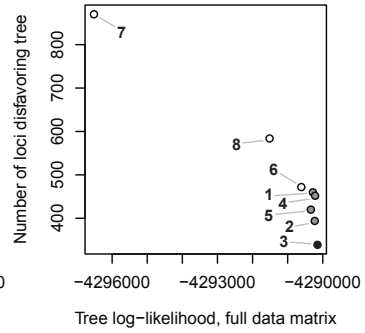
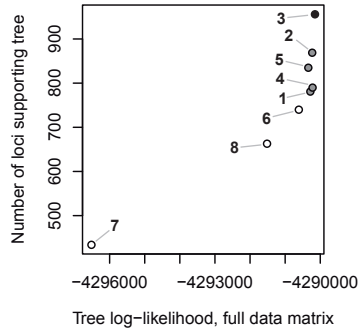
**c84m4**



**c85m4**



**c87m4**



**c92m4**

